Biophysical Studies on DNA Binding and Transcriptional Activities of Myc-Max-Mad Network

By

Anamika Banerjee

A dissertation submitted to the Graduate Faculty in Biochemistry in partial fulfillment of the requirements of the degree of Doctor of Philosophy,
The City University of New York
2006

This manuscript has been read and accepted by the Graduate Faculty in Biochemistry in satisfaction of the dissertation requirements for the degree of Doctor of Philosophy.

_____

(Date) Prof. Dixie. J. Goss
Chair of Examining Committee

_____ _____

(Date) Prof. Lesley Davenport
Executive Officer

Supervisory Committee

_____
(Prof. Yujia Xu)

_____
(Prof. Peter Lipke)

_____
(Prof. Lesley Davenport)

_____
(Prof. William Sweeney)

Abstract

Biophysical Studies on DNA Binding and Transcriptional Activities of Myc-Max-Mad Network

by

Anamika Banerjee

Advisor: Professor Dixie. J. Goss

The members of the Myc/Max/Mad network comprise a wide range of eukaryotic transcription factors. Max is at the center of this network and can initiate activation or repression of transcription depending on whether its heterodimeric partner is Myc or Mad The consensus sequence on the promoter DNA recognized by Myc-Max-Mad network of proteins is a hexameric palindrome CACGTG, also called an E Box.

Fluorescence anisotropy has been used to determine the dissociation constants for DNA-protein and protein-protein interactions of this pathway. These data indicates that Max has higher affinity for DNA binding, however the heterodimeric partner of Max confers specificity of binding. At the level of protein-protein interactions, Myc-Max forms the most stable dimer followed by Mad-Max and Max-Max. These proteins might follow either a monomeric or a dimeric pathway to assemble on DNA. Investigation of the entire thermodynamic cycle of monomer-dimer pathway revealed that the equilibrium constants for first monomer binding to DNA is ~10nM, while the second monomer binding equilibrium is ~2-5μM. This reduced binding affinity of the second monomer may result from a conformational change that monomers are believed to undergo upon binding and also might be essential for reassortment of Max's partner.

The effect of poly ions on protein dimerization and the temperature dependence of this effect were investigated. Negatively charged polymers like poly-L-Glutamic acid reduced the K_{ds} for all three protein-protein dimers. Determination of the thermodynamic parameters both in the absence and in the presence of negative polymers, shows that the protein-protein interaction is characterized by negative favorable enthalpy and negative unfavorable entropy.

Fluorescence Resonance Energy Transfer (FRET) of DNA labeled at either terminus was used to investigate change in DNA conformation upon binding of these homo or heterodimers. The results indicate that only Max binding can bend DNA (~65º) by asymmetric neutralization of charges on DNA's phosphate backbone, but the other two heterodimers Myc-Max and Mad-Max cannot. Myc-Max has additional contacts with the phosphate backbone through residues specific to Myc. The contacts are absent in Max-Max-DNA complex. It is possible that these contacts are reason that DNA does not under go conformation change due to binding of the heterodimers. Finally it was shown that binding affinity of Max increased ~15 fold towards prebent DNA.

Acknowledgements:

My earnest gratitude goes to my thesis advisor Prof. Dixie. J. Goss for giving me the opportunity to work in her laboratory and advising me. Her excellent mentoring has enabled me to learn scores of things related to Biochemistry in last five years and also helped me to take my research project towards a definite direction. I am grateful to my thesis committee members Prof. Yujia Xu, Prof. Lesley Davenport, Prof. William Sweeney, Prof. Peter Lipke for their valuable suggestions and comments, which contributed immensely in my work. My thanks to Prof. Tatyana Polenova, from whom I always got suggestions whenever I had asked for, despite of her very busy schedule and distant location. I do not really know how to acknowledge thanks and gratitude to my Graduate advisor Prof. Klaus Grohmann without whom this long five years journey towards a PhD degree would have been extremely difficult.

I consider myself very fortunate to get a husband like Ajit who has been always by my side and helped me in every possible way to make my work a success.

My mother-in-law's incredible positive attitude towards life inspite of her serious illness has taught me to sustain and get over through the most frustrating moments of my career.

Thanks to the rest of my in-laws family for their continuous support and encouragement. I know my brother-in-law Anil, sister-in-law Mamta and nephew Babi would be specially happy to see me getting this PhD degree. My family back at Calcutta, my Aunts, Uncles, Cousins, especially Tina and Rajat, this thesis would not have been possible if all of you were not there.

My special thanks to Department of Biophysics and Molecular Biology, University of Calcutta, India, where I did my Masters for their excellent training and guidance.

I would like to thank my lab mates and colleagues Dr. Brian Hu, Dr. Diana Friedland, Dr. John Trujillo, Dr. Mateen Khan, Dr. Lou, Dr. Li, Dr. Sibnath Ray, Artem, Ozgur, Hassan, Reena, from whom I learnt so many things Thanks to my friends at Hunter Chemistry department specially Amanda, Diana Samaroo, Nala, Mirella, Tony, Sunej and Fatou.

I would like to take this opportunity to thank Prof. Horst Schulz, the former executive Officer of Biochemistry program CUNY and the current executive officer Prof. Lesley Davenport for accepting me in the Biochemistry program and for enabling me to finish my study. My thanks to our program secretary Judy Li and also to the office of International Students.

I would like to mention my son Aadvik who has made this pursuit for a doctorate degree meaningful in his own little but very precious way.

“Miles to go before I sleep” were favorite lines of my father, without whose inspiration, support and encouragement, my pursuit towards a career in science would not have even begun. My greatest grief and frustration in life is probably that my father could not live through to see me completing my studies. Though I am approaching the end towards the journey in my PhD career, however my promise to him is “miles to go before I sleep”.

Lastly I would like to mention my mother, who waited so patiently, through her own losses and grief to see me graduating. It would have been absolutely impossible for me to finish my thesis if she was not there sharing my responsibilities and sufferings whenever I needed, and constantly encouraging me to move forward, come what may.

This Thesis is dedicated to my parents.

Table of Content

Lists of Abbreviations:

Max	Myc activating factor X
Mad	Max Dimerizer
E BOX	Enhancer Box
HAT	Histone Acetyl Transferase
HDAC	histone deacetylases
hGCN	Human General Control of Amino acids Synthesis
TRRAP	Transformation/Transcription Associated Domain Protein
TAD	Trans Activation Domain
GST	Glutathione Sulfur Transferase
FITC	Fluorescein iso-thiocyanate
ROX	Carboxy-X-Rhodamine
TAMRA	Carboxy Tetramethyl Rhodamine
TRITC	Tetramethyl Rhodamine iso-thiocyanate
FRET	Fluorescence Resonance Energy Transfer
MLP	Major Late Promoter
LCR	Locus Control Region
mLCR	Mutated Locus Control Region
A Tract	Adenine Tract

1.0 Introduction

Initiation of transcription requires the ordered assembly of transcription factors, architectural proteins and template DNA. Many of the transcription factors bind DNA as dimers, and it appears that dimerization through switching between homo- and heterodimeric structures provides a means for diverse target site recognition and function with the least investment of the genome (1). Myc, Max and Mad are three such transcription modulators that bind DNA as dimers. These phospho-proteins belong to a subset of proteins having a c-terminal basic-helix-loop-helix-leucine zipper (b/HLH/z) motif (2).

Interest in the Max network grew out of studies on the Myc oncogene family. Over expression of any of the members of this family, N-Myc, L-Myc and the cellular homolog c-Myc, is correlated with cell proliferation (2). The presence of an N-terminal transactivation domain (TAD) (3) and a C-terminal b/HLH/z domain (4) in c-Myc led to the assumption that this protein would bind DNA as a dimer. However, its poor homodimerization and DNA binding ability at physiological concentrations initiated a search for a heterodimerization partner, eventually leading to the discovery of Max or Myc activating factor X (5). Max is a b/HLH/z protein similar to Myc, lacking the transactivation domain. Max was found to bind specifically with Myc family proteins forming heterodimers and recognizing the promoter hexameric palindromic sequence CACGTG (E-box) (5).

The fact that Max is expressed even in the absence of Myc prompted researchers to search for new Max interacting proteins and led to the discovery of Mad family of

proteins consisting of Mad1, Mxi1, Mad3 and Mad4 (6-8). All of these proteins are similar to Myc in the sense that they homodimerize and bind DNA poorly, however their binding affinities to E Box containing DNA are enhanced when they heterodimerize with Max.

1.0a Myc: c-Myc originally got its name from the ability to cause *my*elo*cy*tomatosis in susceptible animals and cultured cells (9) and was discovered as a protooncogene from avian myelocytoma virus. Myc family proteins have been implicated in cell proliferation, differentiation, and neoplasia. Myc-Max heterodimers recognize the E-box sequence CACGTG (as well as related non-canonical sites) and activate transcription from synthetic reporter genes containing more than one binding sites in mammalian cells, as well as in yeast (10). The effects of Myc on cell proliferation and apoptosis are negated by mutations in the Myc transactivation region, or in the b\HLH\Z domain which is required for association with Max and DNA, indicating a tight linkage between its transcriptional and biological activities (10). It has been established that for transcriptional activity of c-Myc, both its structural organization and association with other proteins are important. The N-terminal transactivating domain of the protein constitute MBI, Myc box 1; MBII, Myc box 2; and NLS, nuclear localization signal; while the C-terminal region has the following sub-domain BR, basic region; HLH, helix-loop-helix; and the LZ, leucine zipper domain (2).

Myc-Max heterodimers activate transcription by recruiting HAT's (Histone acetylase) via TRRAP (Transformation/transcription associated domain protein). This leads to the acetylation of histone tails and the opening of local chromatin structure (11, 12).

However Myc does not act only as a transcription activator only. It has been observed that high levels of Myc expression in transformed cell lines is correlated with down-regulation of specific mRNAs encoding cell surface proteins such as the class I HLA molecules in melanoma cells, the 3 -1 integrin in neuroblastomas and the LFA-1 (L -2 integrin) cell adhesion protein in transformed B cells as well as H-ferritin (2 and the ref therein). More recently a DNA element required for Myc-mediated repression has been demonstrated to lie within the promoters of repressed target genes, indicating that Myc repression is likely mediated at the transcriptional level (12). MBII and the region of Myc spanning residues (96-106) appear to be required for down-regulation of such mRNAs. As a result of these diverse activities at target genes, Myc affects proliferation, cell cycle, growth, immortalization, and apoptosis.

1.0b Max: In 1990, Elizabeth Blackwood and R.N. Eisenmann (13) used the bHLH-Zip region of c-Myc to screen a complementary DNA (cDNA) expression library, and identified a bHLH/zip protein, termed Max. Max specifically associated with c-Myc, N-Myc, and L-Myc proteins, but not with a number of other bHLH, bZip, or bHLH/zip proteins. The interaction between Max and c-Myc was dependent on the integrity of the c-Myc HLH-Zip domain, but not on the basic region or other sequences outside the domain. Max is a b/HLH/z protein similar to Myc, but lacks the transctivation domain. Binding of Myc-Max to the E-Box activates transcription of a series of genes related to growth, cell cycle, and apoptosis (14). Max can homodimerize and bind DNA. Since expression of Max is ubiquitous, a search for Max-interacting proteins by use of expression cloning and two hybrid screens led to the discovery of the whole network of proteins, Mad1, Mad3, Mad4, Mxi1, Mnt and Mga and more recently MondoA,

WBSCR14 all of which use their b/HLH/z domains to form heterdimers with Max, bind to specific DNA sequences and modulate transcriptional activities (2).

In contrast to cell proliferation caused by c-Myc, in absence of c-Myc over expression of Max in stably transfected human B-lymphoblastoid cell lines cause growth inhibition (15). This result initiated the studies on the role of Max as a transcription repressor, without any definite answer till date (2). Max is constitutively expressed and is very stable compared to the short half-lives and regulated expression of its other partners.

1.0c Mad: To determine whether Max mediates the function of regulatory proteins other than Myc, Ayer et al (16) screened a lambda gt11 expression library with radiolabeled Max protein. They identified one cDNA encoding a new member of the b/HLH/zip protein family, which they named Mad or Max dimerizer. Mad like Myc homodimerizes poorly but binds Max, forming a sequence-specific DNA binding complex with properties very similar to those of Myc-Max. Both Myc-Max and Mad-Max heterocomplexes are favored over Max homodimers at equilibrium, and unlike Max homodimers, the DNA binding activity of the heterodimers is unaffected by CKII phosphorylation. Mad does not associate with Myc or with representative bHLH, bZip, or b/HLH/zip proteins. The same study (6), substantiated by further investigations by others (2 and ref therein) suggested that Myc-Max and Mad-Max complexes have opposing functions in transcription and that Max plays a central role in this network of transcription factors (15). Mad 1, Mad 3, Mad 4 and Mxi1 constitute the Mad family of proteins. Studies of the Mad family of proteins reveal that in a wide range of cell types an increase in Mad mRNA level is associated with terminal differentiation. Mad also blocks

proliferation and inhibits transformation. Mad-Max represses gene transcription by associating with the mSin3 corepressor complex via histone deacetylation (2, 17).

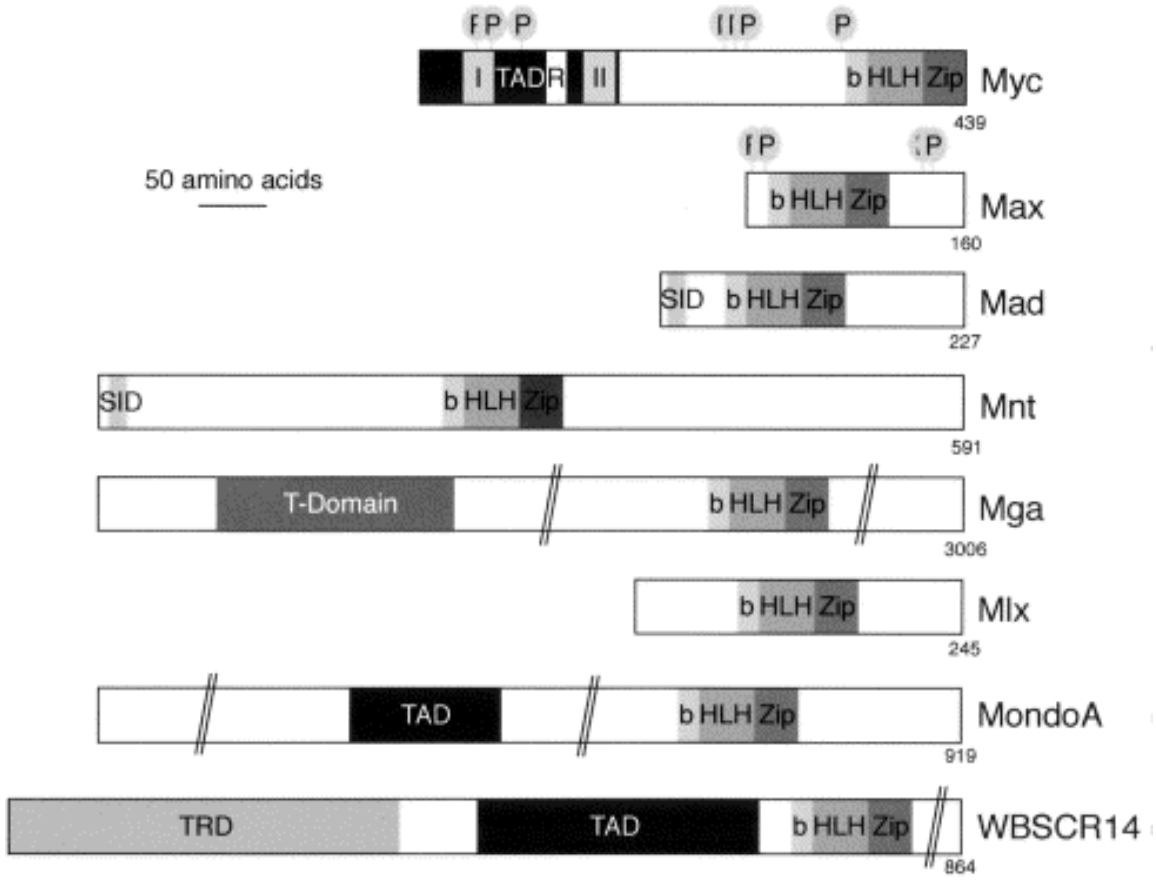

Figure: 1 Structure-function schematic of components of the Myc/Max/Mad network

The known functional domains of different network components are summarized. Information regarding the expression and the loss of function phenotypes, as far as defined, is indicated.

TAD: transactivation domain;

I: Myc box I;

II: Myc box II;

b: basic region;

R: region involved in repression;

HLH: helix-loop-helix domain;

Zip: leucine zipper domain;

SID: mSin3-interaction domain;

T-Domain: T-box DNA binding domain;

TRD: transrepression domain;

P: position of known phosphorylation sites.

The numbers refer to amino acids of the human proteins.

1.0d Myc-Max-Mad Structural Organization: The X-ray structure of the b/HLH/z domain of Max homodimer bound to an E-box, derived from the Adenovirus major late promoter, established the structural bases for DNA recognition by b/HLH/z proteins (18). The structure (Figure 2) revealed that Max dimerizes to form an asymmetric, parallel left-handed four-helix bundle composed of two pairs of right-handed helices (b-H1 and H2-Z). The basic region projects from the N-terminal face of the four-helix bundle and interacts with DNA via sequence-specific contacts to the DNA- major groove edges of base pairs comprising the E box. C-terminal extensions of two helices form a left- handed coiled-coil or leucine zipper. Using synthetically ligated heterodimers Nair et al (19) solved the crystal structures of Myc-Max and Mad-Max bHLHZ bound to cognate DNA sequence. The Myc-Max structure however, was reported to be a bivalent heterotetramer.

Identical amino acid contacts are found to dictate protein-DNA recognition in all three proteins dimers. His28, Glu32 and Arg36 in Max, His359, Glu363 and Arg367 in Myc and His61, Glu65 and Arg69 in Mad are the residues, which make sequence specific contacts with the E Box. In terms of protein-protein interactions the leucine zipper domain is responsible for dimerization specificity. Gln91, Asn92 in Max, Arg23 and 424 in Myc and Glu125 in Mad are observed to be important for dimerization.

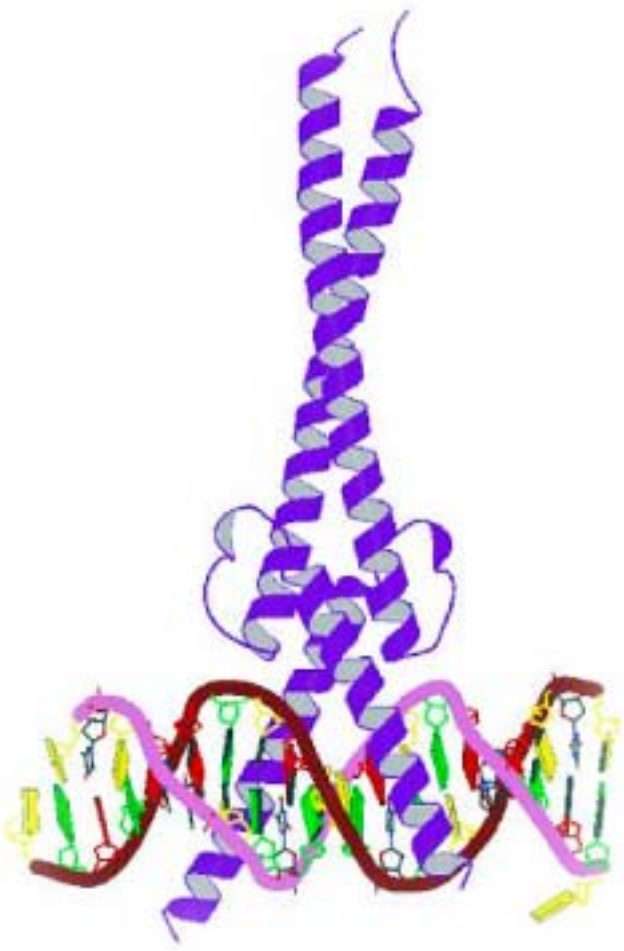

Figure 2. The structure of the Myc-Max heterodimer binding with 19-mer DNA oligos with E-Box sequence obtained from X-ray diffraction by S. K. Nair and S. K. Burley (20)**.**

This crystal structure (Figure 2) only contains the Max HLH domain (23-102) (80aa) and the c-Myc HLH domain (353-434) (82aa), with the binding of the DNA oligonucleotides 5'CGAGTAGCAC GTGCTACTC3' (sequence of complement chain not shown), containing the E-Box CACGTG sequence. The resolution was 1.80Å.

1.0 E-Box: E-Boxes were discovered as cis acting DNA elements, an IgH enhancer, which seems to regulate the transcription of immunoglobulin heavy chain (IgH) gene. Using in vivo methylation, a number of such elements were discovered in IgH and kappa-light chain enhancers, which shared a hexanucleotide core signature sequence CANNTG. There are altogether five E-Box elements in IgH and three canonical elements in kappa light chain (21). Subsequently E-Boxes have been discovered in promoters and enhancers of sequences that regulate gene expression in muscle and neurons. The CACGTG E-Box sequence is a class A E-box element in contrast to the class B, which is CAGCTG. A single amino acid residue is responsible for b/HLH/z family proteins distinguishing class A from class B E-Boxes (2, 21).

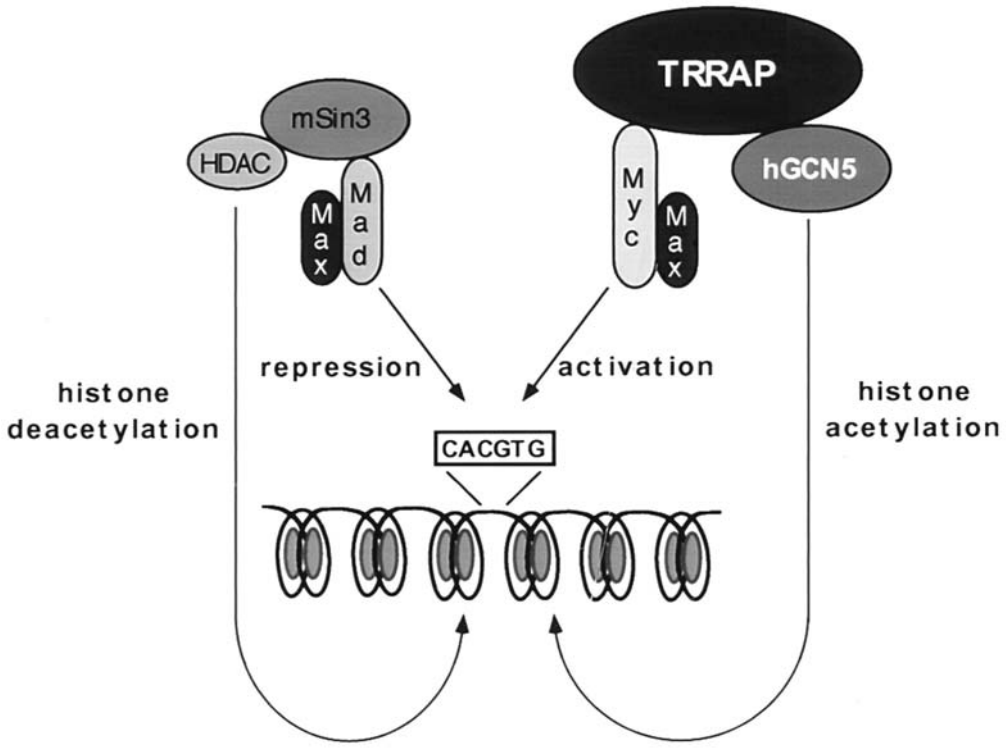

Figure. 3 Model of the opposing biochemical functions of c-Myc and Mad suggest by S. B. McMahon, M. A Wood and M. D. Cole (12)

Figure 3 demonstrates that c-Myc, through its essential cofactor TRRAP, recruits the HAT hGCN5 and suggests a potential biochemical basis for antagonistic biological functions of c-Myc and Mad. In this model, c-Myc-Max heterodimers activate transcription of target genes by recruitment of TRRAP and a HAT such as hGCN5. HAT activity results in nucleosomal remodeling at the target gene loci, allowing more efficient transcription. Following displacement of Myc-Max dimers from their cognate DNA recognition element, Mad-Max dimers recruit deacetylase activity to these sites, which in

turn removes the acetyl groups from histones in nearby nucleosomes. This process facilitates chromatin condensation and consequently transcriptional repression. (2)

Research in last 10-12 years has provided us with considerable information on the mechanisms of function of these important bHLHZip family of transcription factors, however unanswered questions remain about the underlying the biological function and molecular mode of action of the Myc-Max-Mad network. The aim of this research project is to gain further insights into the molecular mechanism of action of the c-Myc-Max-Mad proteins by application of biochemical and biophysical techniques.

1.0f Overview of the Project:

1. c-Myc, Max and Mad proteins were purified from clones using different chromatographic techniques including ion exchange, GST affinity, and nickel affinity chromatography.
2. The b/HLH/z domain of c-Myc protein was subcloned with a thrombin cleavage site in the GST vector in order to obtain the c-Myc92 free from the fusion protein GST.
3. Target DNA sequences of c-Myc-Max-Mad were designed and labeled with different fluorophores: FITC, ROX, TAMRA.
4. Max was labeled at the N-terminus by TRITC.
5. Study of the protein-protein and protein-DNA binding interactions of Max homodimer, Myc-Max and Mad-Max heterodimers with fluorescently labeled oligos were monitored by fluorescence anisotropy..
6. Effect of polyions on dimerization of Max-Max, Max-Myc and Max-Mad were observed by fluorescence anisotropy.

7. Fluorescence resonance energy transfer (FRET) was used to study the DNA conformation change due to binding of homodimers or heterodimers on DNA.

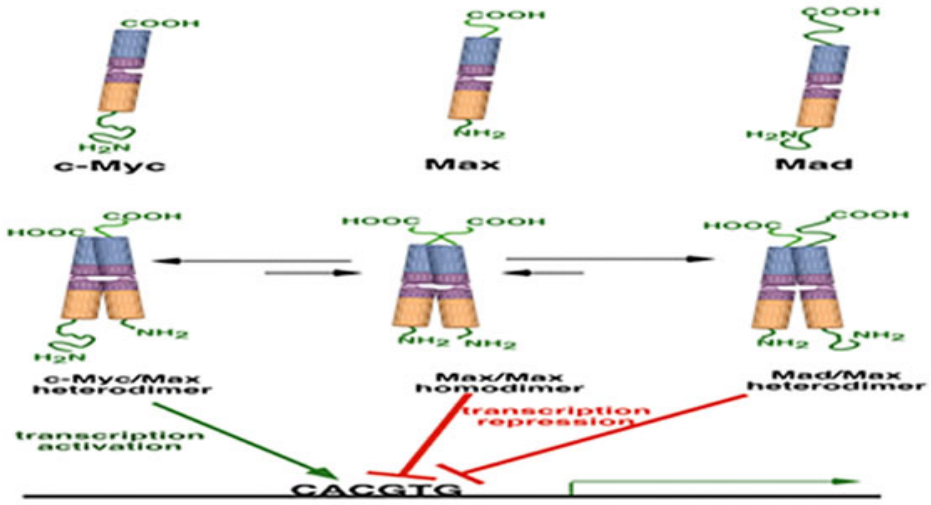

Figure 4. Diagram of the binding model of Max homodimer, Max/c-Myc heterodimer or Max/Mad heterodimer with DNA CACGTG element.

The model in Figure 4 implies that Myc-Max, Max-Max, and Mad/Mnt-Max complexes exist in equilibrium and that shifts in this equilibrium dictate whether transcription of target genes containing CACGTG elements is activated or repressed.

1.0g Fluorescence Anisotropy Measurements

Fluorescence is the result of a three-stage process that occurs in certain molecules (generally polyaromatic hydrocarbons or heterocycles) called fluorophores or fluorescent dyes. A photon of energy $h\nu_{ex}$ is supplied by an external source such as an incandescent lamp or a laser and absorbed by the fluorophore, creating an excited electronic singlet state (S_1'). The excited state exists for a finite time (typically 1–10 nanoseconds). During

this time, the fluorophore undergoes conformational changes and is also subject to a multitude of possible interactions with its molecular environment. These processes have two important consequences. First, the energy of S_1' is partially dissipated, yielding a relaxed singlet excited state (S_1) from which fluorescence emission originates. Second, not all the molecules initially excited by absorption return to the ground state (S_0) by fluorescence emission. Other processes such as collisional quenching, fluorescence resonance energy transfer (FRET) and intersystem crossing may also depopulate S_1. The fluorescence quantum yield, which is the ratio of the number of fluorescence photons emitted to the number of photons absorbed, is a measure of the relative extent to which these processes occur. A photon of energy $h\nu_{em}$ is emitted, returning the fluorophore to its ground state S_0. Due to energy dissipation during the excited-state lifetime, the energy of this photon is lower and therefore of longer wavelength than the excitation photon $h\nu_{ex}$ (38).

The fluorescence measurement can be limited to only certain directions by measuring the polarized fluorescence signal change. Anisotropy is used to calculate the extent of polarization. The anisotropy of fluorescence (r) is determined from the equation 1:

$$r = (I_{//} - I_{\perp}) / (I_{//} + 2I_{\perp}) \qquad (1)$$

Where $I_{//}$ and $I_{\perp}$ are the parallel and perpendicular fluorescence emission intensities, respectively. Anisotropy measurements are based on the average angular displacement that a fluorophore undergoes from the absorption to the emission of the photons. The change in the anisotropy will be observed when there is a change in the environment, such as a ligand binding to the fluorescent molecule, which will cause a reorientation of the fluorophore.

In our experiments, when the labeled proteins or labeled DNAs were titrated with unlabeled proteins, such interaction with the fluorescent molecules caused the anisotropy value to change. The protein-protein and protein-DNA binding equilibria were measured by monitoring the fluorescence anisotropy change of the fluorophore labeled free molecules and their protein or DNA bound states (22, 25).

1.0h Fluorescence Resonance Energy Transfer

Fluorescence resonance energy transfer (FRET) (22) is a distance-dependent interaction between the electronic excited states of two dye molecules in which excitation is transferred from a donor molecule to an acceptor molecule without emission of a photon. The efficiency of the transfer (E_{FRET}) depends inversely on the sixth power of the distance separating the fluorophores and is given by

$$E_{FRET} = 1/[1+(R/R_0)^6] \qquad (2)$$

Where R is the scalar distance between the fluorophores and R_0 is the characteristic Forster distance for the donor-acceptor combination at which E_{FRET} equals 0.5. by FRET. At R_o, there is an equal probability for resonance energy transfer and the radiative emission of a photon. The magnitude of Ro is dependent of the spectral properties of the donor and acceptor:

$$Ro = [8.8*1023K^2n^{-4}Q_d J]^{1/6} \text{ (Angstrom)} \quad (3)$$

where

k^2 or kappa square = dipole orientation factor, a function of donor emission transition moment and the acceptor absorption transition moment (range 0 to 4, generally $k^2 = 2/3$ is assumed)

Q_d = fluorescence quantum yield of the donor in the absence of acceptor

n = refractive index of the medium which is generally assumed to be 1.4 (range 1.33-1.6) for proteins.

J = spectral overlap integral which represents the degree of overlap between the donor fluorescence spectrum and the acceptor absorption spectrum.

The donor and acceptor must be within $0.5R_0$ -$1.5R_0$ from each other. These measurements give the average distance between the two fluorophores. The typical value of R at which important information on macromolecular distance is available ranges from 10-80Å.

Chapter 1

1.1 Fluorescence Anisotropy Study to Determine DNA-Protein and Protein-Protein Interactions in the Myc/Max/Mad Network.

While there have been a number of studies on the DNA sequence preferences of the b/HLH/z proteins, there have been very little quantitative data on protein-protein and protein-DNA interactions. An understanding of protein interactions with DNA is the first step in understanding the mechanism of action of this important biological process.

In this work, we have investigated the binding of Max, Max-Myc, and Max-Mad1 to DNA oligonucleotides containing the E-box and to other oligonucleotides with various base substitutions. We have determined protein-protein interactions as well. The results from direct fluorescence anisotropy titration measurements showed a single binding mode for Max binding to DNA that is attributed to a dimer-DNA interaction.

The equilibrium constants for the complete thermodynamic cycle for assembly of protein dimer-DNA from monomer and DNA have been determined. These data give insight into the assembly of the protein-DNA scaffolding and serve as the basis to investigate the effects of other members of this complex network.

Fluorescence polarization and anisotropy have been used extensively to monitor protein - protein and protein-DNA interactions (22 and references cited therein).

For the simple binding one can obtain the theoretical equation for the K_d (dissociation constant) between p`rotein-protein and Protein-DNA with following:

For a simple binding reaction A + B ↔ C The dissociation constant, K_d, is defined as:

$$K_d = \frac{[A][B]}{[C]} \qquad (4)$$

Here, $[A] = [A]_t - [C]$

$[B] = [B]_t - [C]$

$$\text{So, } Kd = \frac{([A]_t - [C])([B]_t - [C])}{[C]} \quad (4a)$$

$$[C]^2 - ([A]_t + [B]_t + K_d)[C] + [A]_t[B]_t = 0 \quad (4b)$$

$$[C] = \frac{\left[([A]_t + [B]_t + K_d) + \sqrt{([A]_t + [B]_t + K_d)^2 + 4[A]_t[B]_t}\right]}{2} \quad (4c)$$

Since the normalized anisotropy change $\Delta r = \frac{(r - r_0)}{(r_\infty - r_0)} = \frac{[C]}{[A]_t}$, the [C] in the above solution is replaced by $\Delta r \times [A]_t$

Therefore,

$$\Delta r = \frac{\left[([A]_t + [B]_t + K_d) + \sqrt{([A]_t + [B]_t + K_d)^2 + 4[A]_t[B]_t}\right][A]_t}{2} \quad (5)$$

[A]: concentration of chemical A at equilibrium

[B]: concentration of chemical B at equilibrium

[C]: concentration of chemical C at equilibrium

$[A]_t$: totaling concentration of chemical A

$[B]_t$: totaling concentration of chemical B

r_0 : initial anisotropy signal

r: anisotropy signal in each titration

r_∞: the maximum anisotropy signal (saturation state)

In the expression above, Δr and $[B]_t$ are the x and y parameters with two variables with two parameters, $[A]_t$ and K_d. By inputting and running this equation in KaleidaGraph (Synergy 2.6) data analysis program, the dissociation constant for each interaction can be obtained. The data were fit to a single equilibrium constant K_d. (22, 23, 25).

Thermodynamic parameters for Max-TRITC binding to unlabeled Max, Myc or Mad were analyzed according to van't Hoff isobaric equation assuming that $\Delta H°$ and $\Delta S°$ remain unchanged over the temperature range studied:

$\Delta G° = -RT\ln K_{eq} = \Delta H° - T\Delta S°$ *(6)*

1.2 Materials and Methods

1.2a Protein purification.

The expression vectors Max/pET3a and c-Myc/pGex2T were obtained from S.K. Burley, Rockefeller University. The expression vector Mad1/pET30a was constructed (Appendix 1a) using Mad cDNA (purchased from Open Biosystems, Huntsville, AL). A thrombin protease cleavage site was introduced in the c-Myc-GST clone in order to get c-Myc b/HLH/z free from GST (Appendix 1b). The Max, Mad1 and c-Myc proteins were all expressed in *E. coli* BL21-pLys cells containing the DE3 promoter. In order to obtain soluble proteins, Max consisted of amino acids (22-113), c-Myc (aa 347-439) and Mad1 was the full length protein. These constructs contained the functional b/HLH/z domains of the proteins. A brief description of name, molecular weight and types of plasmids used in expression and purification of Myc, Max, and Mad proteins are given in Table 1.

Cells containing pET-Max or pGEX-Myc were selected by colony selection and inoculated into one liter LB media with 50 μg/mL ampicillin. After being grown to 0.6 OD_{600}, the cells were induced with 1 mM isopropyl β-D-thiogalactopyranoside (IPTG) and further incubated for 6 hrs. Cells containing pET-Mad vectors were also selected by colony selection. Ten ml of transformed E. coli cells were inoculated into one liter LB media with 50μg/mL kanamycin and grown to 0.6-0.8 OD_{600}. The cells were induced with IPTG and continued to grow for 6 hours. The pellets were collected by centrifugation for 20 min and 6000 rpm and resuspended in HEPES buffer (pH 7.6) (for Myc PBS, pH 7.4 was used) with protease inhibitor cocktail and lysozyme. The cells were stored on ice for one hour and then sonicated twice for one minute with a 30 sec interval between sonication. The supernatant was used for chromatography and

purification of the proteins. For Mad1 and c-Myc, the pellets were also saved for treatment of inclusion bodies.

The inclusion bodies for Mad1 were washed twice with 10 mL of 20 mM HEPES buffer (pH 7.6) containing 1% triton X100 followed by centrifugation at 18000 rpm for 30 min at 4^0 C. The pellet (inclusion bodies) was dissolved in 2 mL 50 mM HEPES buffer pH 7.6, 6M guanidine HCl, 25 mM DTT and incubated for one hour at 4 ^{0}C. Insoluble material was removed by centrifugation (18000 rpm, 10 min) and the supernatant was diluted into 20 mL cold 50 mM HEPES pH 7.6.

The inclusion bodies for c-Myc were washed as described above for Mad1. The pellet was dissolved in 10 mL PBS Buffer, pH 7.4 containing 1% Triton x-100 and incubated overnight with gentle stirring. Insoluble material was removed as described above and the supernatant was diluted into 20 mL cold 20 mM PBS pH 7.4.

Max was purified by HiTrap SP ionic exchange chromatography using the same protocol as described elsewhere (19,25). c-Myc was purified by GST affinity chromatography (Amersham Biosciences) using 20 mM PBS pH 7.4 as the wash buffer and 50 mM glutathione, 200 mM Tris-HCl pH 8.5 as the elution buffer. Mad1 was purified on Ni^{2+}-His Trap affinity column (Novagen). Depending on the concentration of protein in the sample and the His-bind resin capacity, the proper volume of resin was packed under gravity flow. Resin was washed with 10 volumes of binding buffer (0.5 M NaCl, 20 mM Tris-HCl, 5 mM imidazole, pH 7.9) and the protein samples loaded onto the column. The column was washed with additional binding buffer and 3-10 volumes of wash buffer (0.5 M NaCl, 60 mM imidazole, 20 mM Tris-HCl, pH 7.9) and the protein was eluted with the same buffer containing 1M imidazole. The protein fractions were collected, extensively

dialyzed in HEPES buffer pH 7.6, purity analyzed by SDS-Page, concentrated and the concentrations were determined using a Bio-Rad protein assay kit (Bio-Rad Laboratories, CA, USA).

Protein	***Vector***	**Amino acid residues**	**MW of the purified protein**	**Method of purification**
Max	pET 23	22-113	~10kDa	Cation Exchange Chromatography using a Hi Trap HP column
c-Myc92	pGEX2T	347-439	~10kDa	Affinity Chromatography using GST affinity column from Amersham
Mad	pET30a	Whole length 220 amino acids.	~30kDa	Affinity Chromatography using Nickel affinity column from Novagen

Table 1. Clones, Molecular Weights and the types of chromatography used to purify Myc, Max and Mad

1.2b Fluorescent labeling of Max protein

The N-terminus of Max protein was labeled with tetramethylrhodamine-5-isothiocyanate (5-TRITC). Because 5-TRITC reacts only with uncharged primary amines, under mild conditions, the N-terminus of Max was labeled. Max protein concentration was adjusted to ~ 1.0 mg/mL in 50 mM HEPES buffer (pH 7.6) and a total volume of 5.0 mL. 100 uL of TRITC dissolved in anhydrous DMSO (1.5 mg/mL) was added per one mL of protein solution. The protein-dye mixture was incubated overnight in the dark at 4 ^{0}C with

continuous gentle agitation. Labeled protein was separated from free rhodamine compounds by Sephadex G-15 gel filtration eluted with HEPES buffer. The collected fractions were concentrated with Centricon YM filters (Amicon Corp) by centrifugation for 6 hours at 4000 rpm. The final protein concentration and fluorophore/protein (F/P) ratio was determined by measuring absorbance at 280 nm and 540 nm. The following formula was used to obtain F/P ratios:

$$A_{protein} = A_{280} - A_{540} \times CF \qquad (7)$$

where

$$CF = (A_{280\ free\ dye})/(A_{540\ free\ dye}) = 0.30 \text{ for TRITC} \qquad (8)$$

$$\text{and } [Protein] = A_{protein}/ (1.4 \text{ mg/ml}) \qquad (8a) \text{ and the}$$

$$F/P \text{ ratio} = (MW \times A_{540})/[Protein] \times \varepsilon \qquad (9)$$

was calculated using $\varepsilon = 93000$ for TRITC.

The site of protein labeling was confirmed by enzymatic digestion. Approximately 90% of the protein was labeled (1 dye/monomer). Labeling at sites other than the N-terminus was not detected.

1.2c DNA oligonucleotides

DNA binding was measured using synthetic oligonucleotides purchased from GeneLink (Hawthorne, NY). The 21- or 16-bp oligonucleotides used in this study contained the

sequence derived from the adenovirus major late promoter (MLP) containing the E-box (CACGTG). Sequences with three bases that are different from the MLP sequence are based on the human globin locus control region (LCR) transcription complex which contains the USF binding site. A modified LCR (mLCR) sequence with three other mutations and a base mismatch in the E-box was also used. Three 21-mer oligonucleotides were used to measure the difference in binding for variations in the E-box sequence. The oligonucleotides were hybridized together to form double-stranded DNA before titrations. Equal concentrations (10-20 μM) of labeled oligonucleotides and their unlabeled complements were dissolved in nuclease free water, heated to 75-80 ^{0}for 30 min and allowed to cool slowly overnight. Sequences of the oligonucleotides used are listed below:

Oligonucleotides	DNA sequences (complementary strand not shown)
16-mer MLP	5'TAGGC**<u>CACGTG</u>**ACCGG3'
16-mer LCR	5'TAG*A*C**<u>CAC*C*TG</u>**AC*T*GG3'
16-mer mLCR	5'TAGGC**<u>CACCTG</u>***CC**TC*G3'
21-mer E-Box	5'GTGTAGGC**<u>CACGTG</u>**ACCGGGT3'
21-mer Half-Ebox	5'GTGTAGGC**<u>CA*G*GTG</u>**ACCGGGT3'
21-mer Non-Ebox	5'GTGTAGGC**<u>CA*G*CTG</u>**ACCGGGT3'

Table 2: Sequences of Oligonucleotides used to study protein DNA interactions. E-Boxes or modified E-Boxes are underlined**.**

The DNA oligonucleotides was purchased either as an unlabeled oligonucleotides (and their complements) or with a 5' fluorescein isothiocyanate derivative (Fig 5).

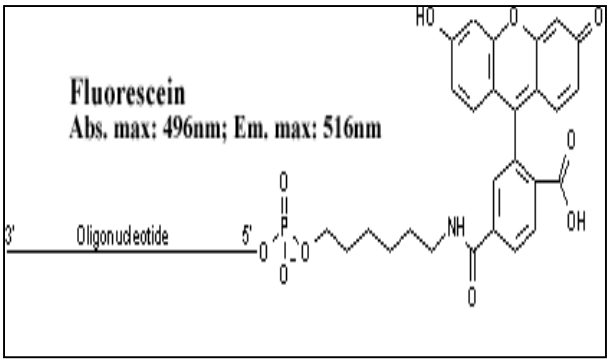

Figure: 5 Fluorescein dye attached to oligonucleotide.

Fluorescence measurements were performed with a SPEX τ2 spectrophotometer, and data were fitted with the KaleidaGraph data analysis program (Synergy 2.6)

1.3 Protein Dimer Binding to DNA Oligonucleotides.

Fluorescently labeled DNA oligonucleotides were titrated with unlabeled protein. The resulting anisotropy change was used to calculate the dissociation equilibrium constant according to equations described previously (*22, 23*). Oligonucleotide concentrations were 15-50 nM. Titrations were carried out in 25 mM HEPES-KOH buffer, pH 7.6, containing 50 mM KCl, 10 mM DTT, 5 mM $MgCl_2$, and 0.5 mM EDTA for heterodimer titrations; Myc or Mad concentrations were in 5-10-fold excess of Max. Max was preincubated with the Myc or Mad protein prior to titration.

1.3a Result:

The binding affinities of Max protein for LCR and MLP DNA oligonucleotides were measured. The MLP sequence was also used in the x-ray crystallographic structure determination of Max_2-DNA (19). The titration data shown in Figure 6 and 7 demonstrate that there are significant differences in the binding affinity of Max protein to MLP and LCR DNA. The specific binding between MLP DNA and Max is about 10-fold higher than the affinity towards LCR DNA and about 100-fold tighter than for the mLCR sequence (Table 3). An interesting observation is that the final anisotropy of the bound DNA is considerably higher for the MLP DNA than for mLCR or LCR DNA (0.223 ± 0.01 and 0.116 ± 0.01, respectively). This suggests that the binding mode may lock the DNA into a more rigid conformation for the specific binding, allowing less rotation even at the terminus where the fluorescent label is attached. This could be accomplished by interactions outside the E-box binding region such as a hydrogen bond between an amino acid in the loop region of the protein and the flanking sequence of the DNA. It is also possible that there could be a charge interaction between an amino acid side chain such as Lys 57 and a residue in the flanking sequence. Hu et al. (25) have determined the pH dependence of the binding between pH 6.5 and 8.5 (data not shown). No significant changes in binding affinity as a function of pH were found. This would indicate that if a charged residue is involved, it does not have a pK near this pH range. Cave et al. (24) used NMR to study Pho4 b/HLH domain binding to E-box and nonspecific DNA. They concluded that there was little difference in protein backbone dynamics, but that the protein may slide along the nonspecific target sequence. Such motion would contribute to a lower overall anisotropy for LCR and mLCR DNA binding.

The data in Figures 6 and 7 show a single binding mode for Max binding to DNA. The Max-DNA binding profiles indicated Max dimer binding to DNA and did not show a biphasic-binding mode, which has been observed with USF (27). USF, another b/HLH/Z protein, recognizes the same E-box sequence and binds as two dimers (homotetramer) to two duplex DNA molecules (or to two E-box sites on the same DNA which forms a loop). It has been shown that Max binds as a dimer to the E-box with each monomer interacting with one half of the E-box (21). Similar binding is observed for the Myc-Max and Max-Mad1 heterodimer binding to E-box DNA. The series of oligonucleotides described in Table 2 as E-box, half-E-Box and non-E-Box were constructed to examine the contribution of each half of the E-box to dimer binding affinity and stability. The non-E-box has only altered the two central bases and is still considered an E-box, however lacking two essential interactions (see below). Table 3 shows the equilibrium dissociation constants and corresponding ΔG values for Max homodimer and the two heterodimers.

Titration experiments have been performed with Max-c-Myc and Max-Mad heterodimers to detect the free energy contribution of their interactions with the same E box, half E box and non-E box DNA sequences. The results showed the similarity in binding between these two heterodimers but very different binding from the Max homodimer (Table 3, Figures 8 and 9). For the heterodimers, the free energy differences between non-specific binding and E-box binding were much larger than for the Max homodimer interacting with DNA. We were unable to accurately measure binding of the heterodimers to the non-E box sequences. These results support the hypothesis that in the Myc/Max/Mad network, Max contributes more to the high binding affinity to the DNA, however recognition of DNA sequences is more likely contributed by Max's partner, Myc or Mad.

These results also support previous studies of binding preference that suggest Myc-Max heterodimers bind only a subset of the sites bound by Max homodimers, due to a differential recognition of the flanking sequences (28-29).

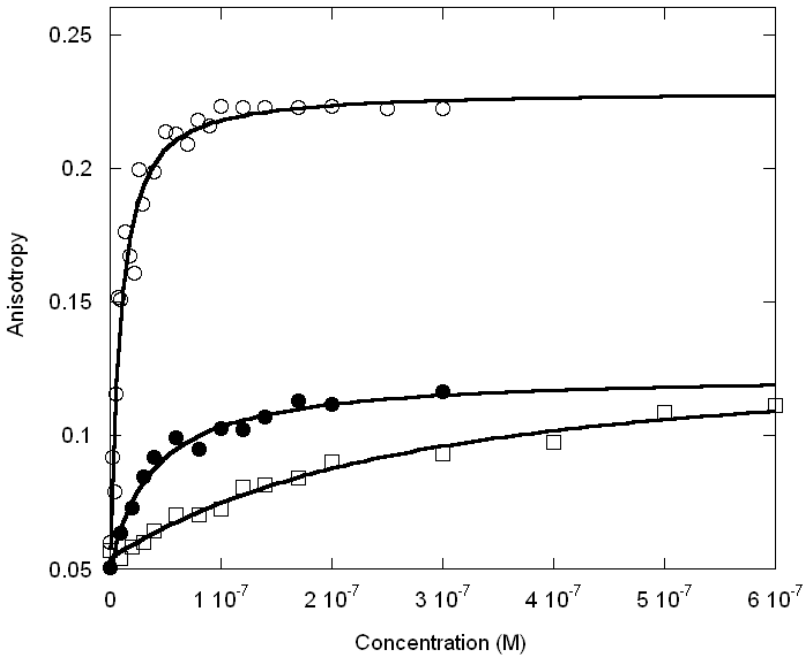

Figure 6 MLP DNA oligonucleotide (O), LCR DNA oligonucleotide (●), and mLCR DNA oligonucleotide (□) titrated with Max protein. The concentration of MLP was 20 nM; the concentrations of LCR and mLCR were 100 nM. Anisotropy change was shown as the *Y* value by increasing the Max protein concentration (*X* value). Oligonucleotides were labeled with FITC at 5' terminus (Excitation at 490 nm and Emission at 520 nm). The temperature was 22 °C. The Buffer used for titration was 7.6 pH HEPES-KOH titration buffer (as described in 1.3). The titration curves indicate stronger binding affinity for MLP than LCR.

Max + DNA of following type	Equilibrium Dissociation constant K_D(nM)
MLP	2.2±0.5
LCR	33.3 ±7.7
mLCR	230 ±10

Table 3: Equilibrium binding constants of Max with MLP, LCR and mLCR DNA oligonucleotides. Experimental conditions were the same as those in Figure 6.

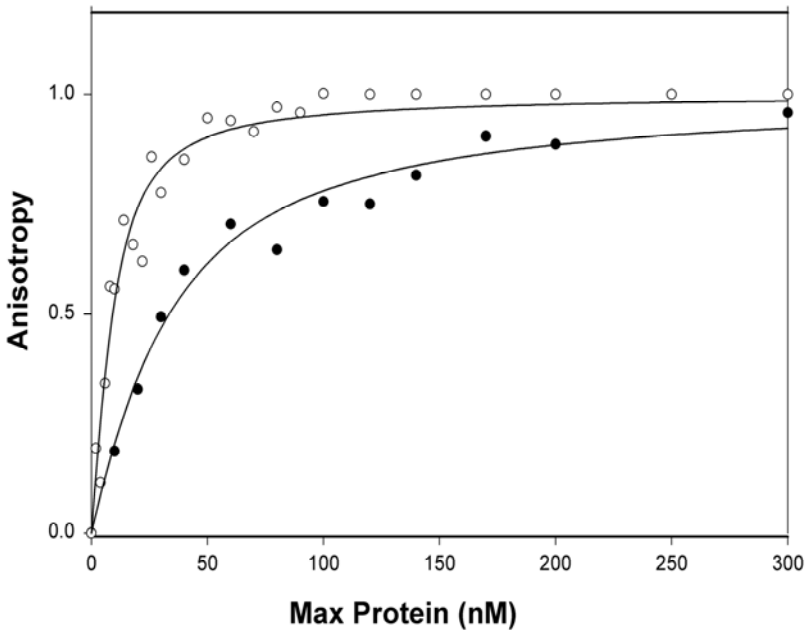

Figure 7: Normalized binding of Max protein to MLP (O) and LCR (b) DNA oligonucleotides. The normalized values represent the fraction bound. Experimental conditions are as described for Fig 6.

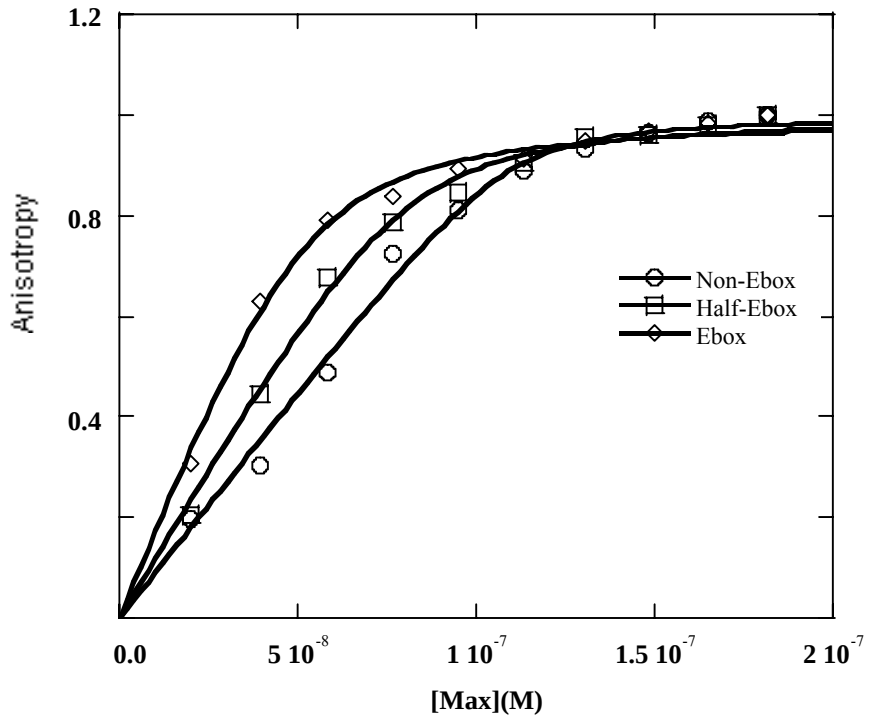

Figure 8 Anisotropy change for the interaction between Max protein and three different oligonucleotides. The concentrations of E-box (◊), half-E-box (□), and non-E-box (O) oligonucleotides were 50 nM. Oligonucleotides were labeled at 5' terminus with FITC (Excitation at 90 nm and Emission at 520 nm). The temperature was 21 °C. The buffer used was HEPES-KOH titration buffer (as described in 1.3) pH 7.6 The base sequences for the oligonucleotides are given in Table 2. The equilibrium constants obtained from the anisotropy change are listed in Table 4.

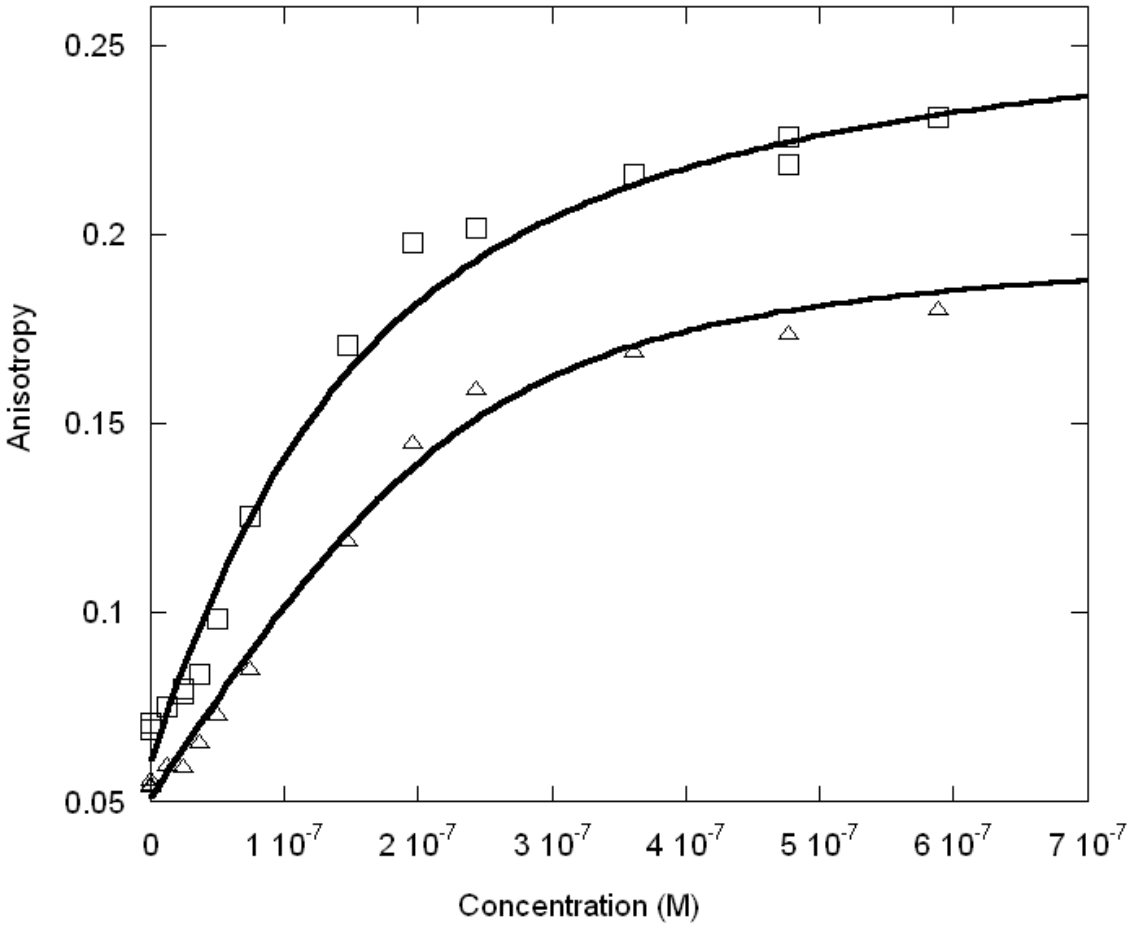

Figure 9 Anisotropy change for the interaction between Myc-Max protein and E-box (□) and half-E-box (Δ) oligonucleotides. The experimental conditions are the same as for Figure 8.

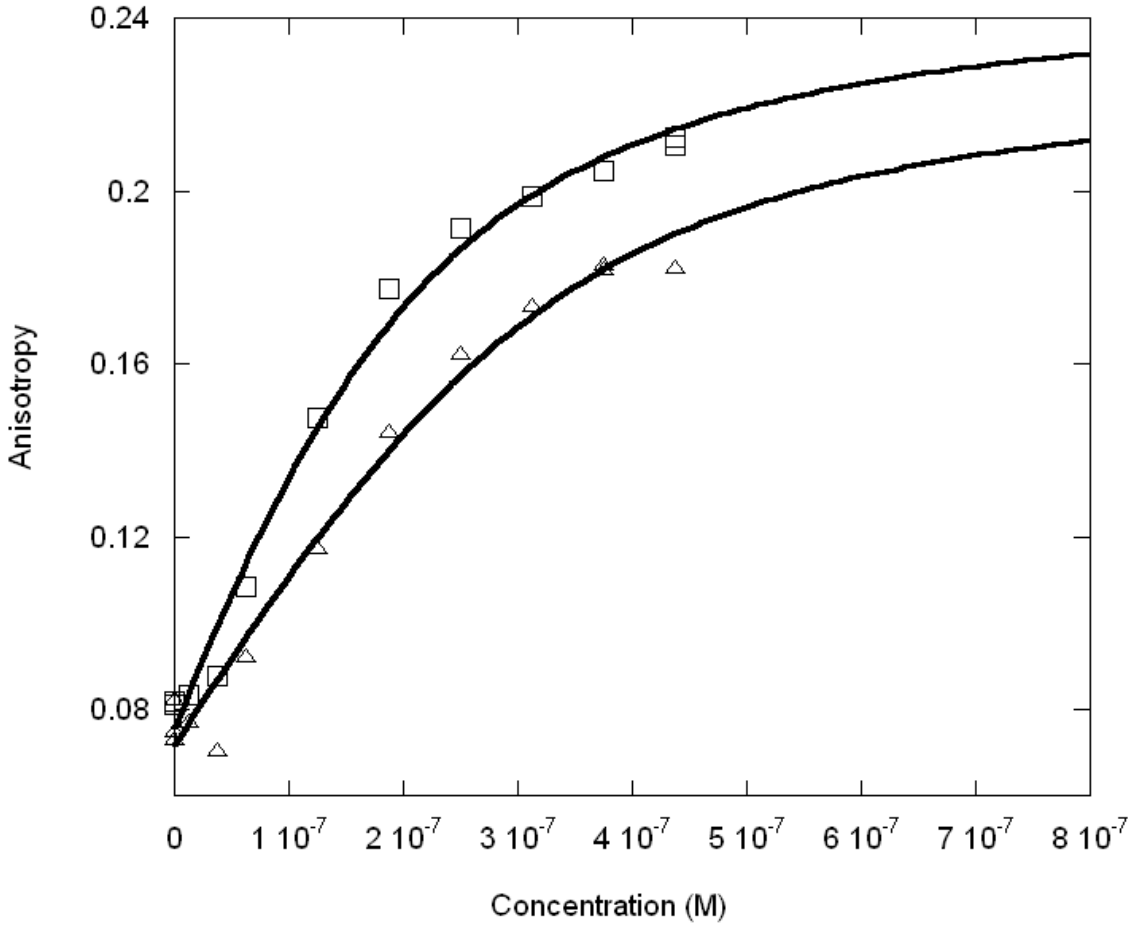

Figure 10 : Anisotropy change for the interaction between Mad-Max protein and E-box (□) and half-E-box (Δ) oligonucleotides. The experimental conditions are the same as for Figure 8.

Oligos (21mers)	Max_2 K_d (nM)	ΔG(kJ)	Max-c-Myc K_d (nM)	ΔG (kJ)	Max-Mad K_d (nM)	ΔG (kJ)
Ebox	19.2±4.4	43.3±0.5	90.5±25.4	39.6±0.8	192±48	37.7±0.6
Half-Ebox	48.7±8.3	41.1±0.3	229±35	37.3±0.3	315±83	36.5±0.6
Non-Ebox	87.0±20	39.0±0.4	------	------	-------	------

Table 4: Dissociation constants (K_d) and ΔG for protein binding with different oligonucleotides

1.4 Myc-Max is a dimer under physiological conditions of study:

Nair and Burley (20) in their crystal structure observed that Myc-Max binds DNA in form of a bivalent tetramer. However other groups (2 and references there in) and our data at physiological concentration supported a dimeric form. In order to confirm this, we compared the anisotropy of Mad-Max dimer and the Myc-Max dimer in which the GST tail is cleaved off. Since anisotropy depends on the rotational relaxation time (22), an increase in molecular weight, such as dimer formation, is expected to increase the anisotropy. If there is no change in fluorescence lifetime and the limiting anisotropy is not reached, the change is directly proportional to the molecular weight change (22, 25). Proteins were purified as described in S ection 2.1a. Max was purified at high concentrations about 5mg/ml and labeled with TRITC (Figure 11) according to the procedure described in Section 2.1c. Myc was purified as a 36 kDa protein fused with 25 kDa GST with a protease cleavage site (Appendix 1.2) and cleaved with thrombin protease to get the ~10kDa b/HLH/z domain of the Myc.

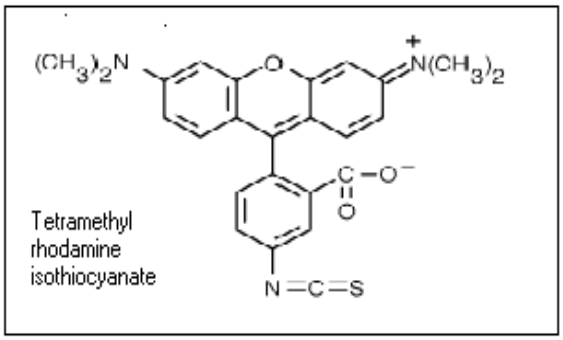

Figure 11 Structure of TRITC used to label Max at the N-terminus

1.4a Results:

When labeled Max was titrated with unlabeled Max, Myc or Mad there was an increase in fluorescence anisotropy as expected. Figure 12 shows the anisotropy change observed. The larger anisotropy change for Mad is due to the larger molecular weight of the heterodimer.

The Max homodimer has a MW of ~ 20 kDa, Myc- Max heterodimer is ~22 kDa, and Mad-Max is ~ 40 kDa. Tetramer formation of Myc-Max as reported from x-ray crystallography (19) would result in substantially higher values for the anisotropy (19). The stoichiometry of these reactions was determined by analysis of the anisotropy, which is related to the molecular weight as described above. When Max was titrated with a larger species (Mad or GST-Myc) the anisotropy was substantially higher. Thus there was no evidence of tetramer formation under these experimental conditions.

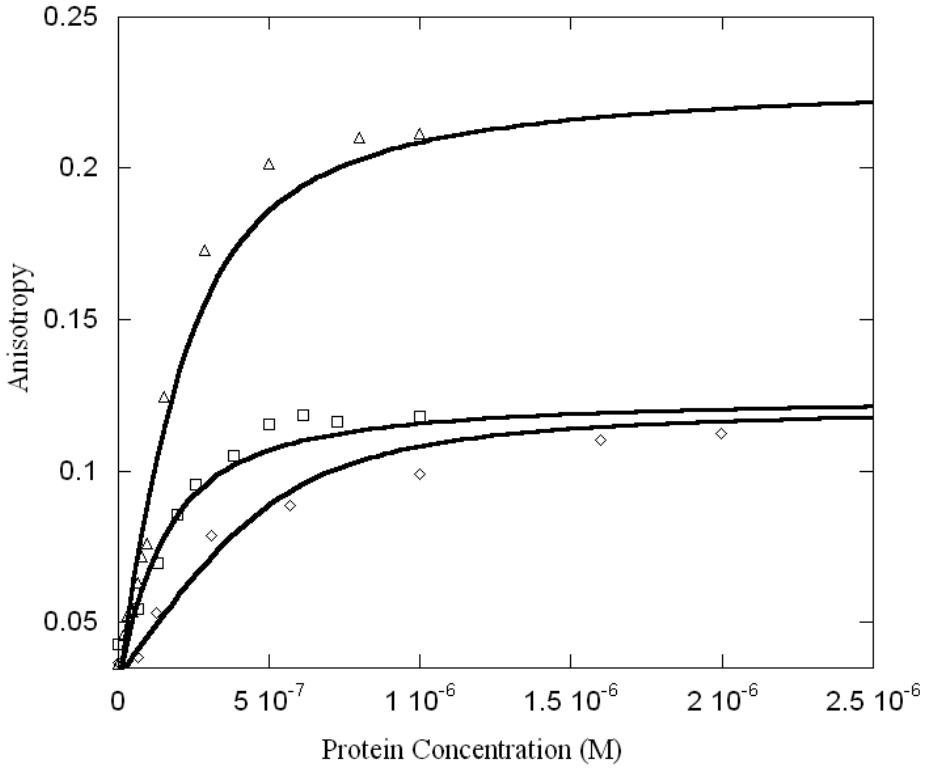

Figure 12: Dimerization of Max-Max (◊), Myc-Max (□), and Mad-Max (Δ). Max was labeled with TRITC (Excitation at 540 nm, and Emission at 576 nm). Labeled Max (100 nM) was titrated with increasing concentrations of unlabeled Max, Myc, or Mad. For these experiments, GST was enzymatically removed from Myc. The temperature was 20 °C. The buffer used was HEPES-KOH titration buffer (as described in section 1.3), pH 7.6. The larger anisotropy change for Mad is attributed to the larger molecular mass.

1.5 Determining the Equilibrium of Monomer-Dimer Pathway

Assembly of the dimer-DNA complex for the Myc/Max/Mad proteins can be described by the cartoon shown in Figure 13.

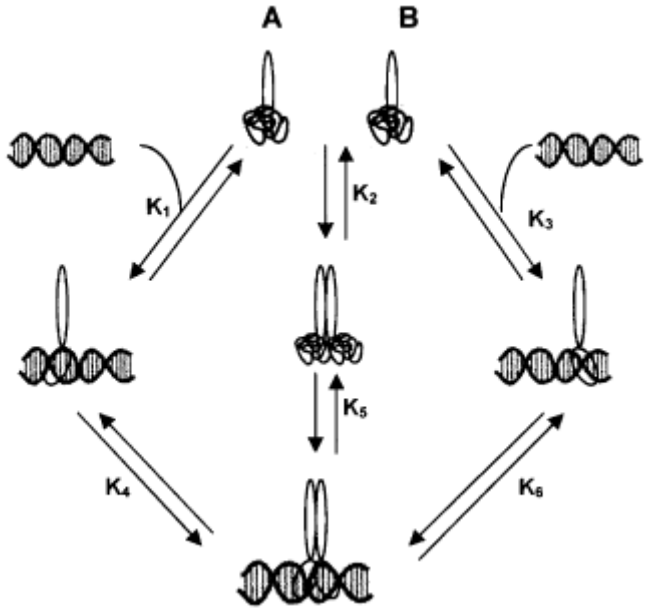

Figure 13: Schematic diagram of monomer, dimer, and DNA interactions.

This cartoon represents the case for heterodimer-DNA formation where A and B are different monomers. The unstructured monomers interact with DNA (K_1, K_3) or each other (K_2). The monomer pathway (K_1, K_4 or K_3, K_6) predicts the sequential addition of the second monomer. (For steps K_4 and K_6, the second monomer is not shown). The dimer binding pathway (K_2, K_5) is also included. In the case of homodimer formation, A and B are identical and therefore $K_1 = K_3$ and $K_4 = K_6$, thus simplifying the scheme. The protein monomer-dimer equilibrium (K_2) is listed in Table 3. Dimer binding to DNA was also determined. For homodimers, it has been reported (2, 15) that neither Myc nor Mad binds DNA very well. Consequently, if a solution is composed

of Max and excess of either Myc or Mad as described in Materials and Methods section 2.1a, the predominant species will be Myc_2 and Max-Myc. Using Myc-Max as an example, data indicate that the Myc-Max monomer-dimer equilibrium constant is around 0.2 micromolar and the Myc-Max-DNA binding is around 5 nanomolar. There is one important observation, however, that will allow us to determine the dimer-DNA equilibrium constant and that is the fact that Myc_2 binds DNA poorly and that Myc forms a homodimer only weakly. We find that by having Max at low nanomolar concentrations and Myc at low micromolar concentration, essentially all of the Max is in the desired Myc-Max complex. At these low concentrations, there is negligible Max dimer present.

1.5a Results.

Given the equilibrium data, assembly of dimer-DNA complexes must follow a monomer pathway because binding to DNA occurs in the nanomolar range and monomer-dimer association occurs in the micromolar range. Therefore, there is virtually no dimer present initially when DNA is titrated with protein and the initial binding must be a monomer. A titration of DNA with low concentrations of Max, followed by Myc yields a fluorescence titration curve shown in Fig. 14.

Considering the thermodynamic cycle given in Figure 13, three equations and four unknowns arise. K_5, the dimer binding to DNA, was determined as described above for both Mad-Max and Myc-Max and the monomer-dimer equilibrium, K_2 was determined for both proteins. By titration of a solution of labeled Max and excess DNA with either Myc or Mad, K_4 was measured and using the formula $K_1=K_2*K_5/K_4$, K_1 was also be obtained. Table 5 gives the relevant equilibrium values for the entire pathway. The values for K_1 obtained by using the Myc equilibrium constants and the Mad equilibrium constants are different by less than a factor of two. This redundancy gives good agreement in the final parameters.

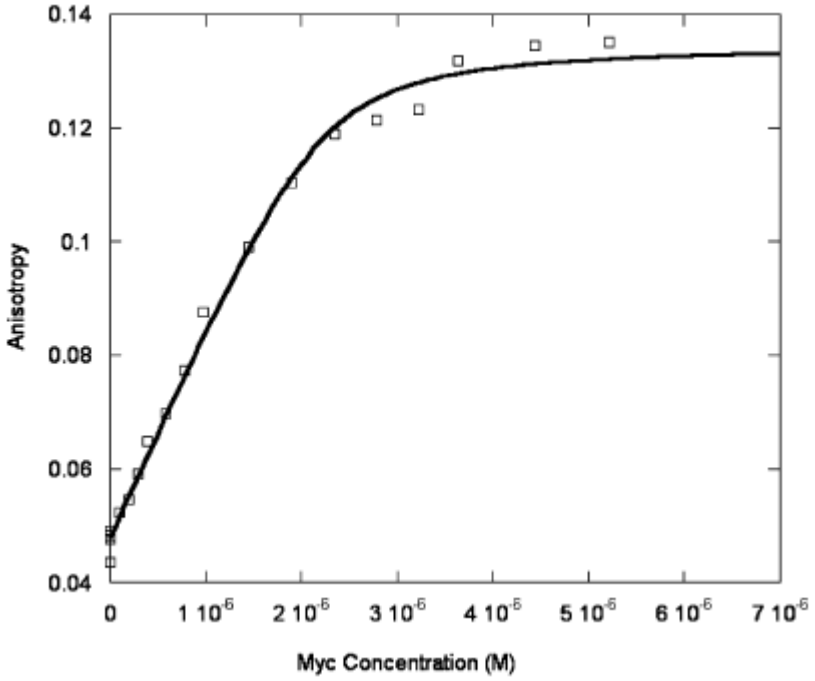

Figure 14: TRITC labeled Max monomer (50 nm) + DNA complex (100 nM) preincubated overnight was titrated with increasing concentrations of Myc protein. Experimental conditions were as described in Figure 12.

Protein	K_1 (K_3) (nM)	K_2 (nM)	K_4 (K_6) (uM)	K_5 (nM)
cMyc	6.8 ± 1.6	176 ± 12	2.2 ± 0.1	84 ± 10
Mad	10.2 ± 1.8	320 ± 25	5.3 ± 0.2	168 ± 14
Max	8.1 ± 1.2	680 ± 44	2.1 ± 0.1	15 ± 2

Table 5. Equilibrium constants for the reactions in Figure 13

Table Footnote

[1]The values for K_1 are for the first Max monomer binding to DNA as calculated from data for the binding of the Myc, Mad, or Max hetero- or homodimer as described in results.

1.6 Thermodynamics of Protein-Protein interactions of cMyc, Max and Mad: Effect of Polyions on Protein dimerization

Previous section and studies by Kohler et al. (1) supports assembly of b/HLH/z proteins through a monomer binding pathway where one monomer binds DNA followed by dimerization with a second monomer on the DNA. However, even in the absence of DNA, Max-Max, Myc-Max and Mad-Max form dimers. Both the homodimer and the heterodimers form an asymmetric parallel left handed four helix bundle consisting of two pairs of right handed α helices H1 and H2 and C-terminal extension of the α helices, the left handed coiled coil leucine zipper (18). Crystal structures of Max homodimer (19), and Myc-Max and Mad-Max heterodimers (20) along with solution NMR data of Myc-Max synthetic leucine zipper dimer (30) confirmed the putative role of LZ in dimerization specificity. LZ is thought to be specifically responsible for molecular recognition.

Crystallographic and NMR (18-19) studies have revealed important data on specific amino acids involved in dimerization of Max-Max, Myc-Max and Mad-Max. Previous sections showed the importance of protein-protein interactions in assembly of the transcription initiation complex. Moreover, the HLH/z domain of Myc-Max is a potential target for inhibitors (19-20). In order to further understand these interactions, binding constants and thermodynamic data have been obtained. In this study, as in Section 1.5, Max was labeled with TRITC and titrated with unlabeled Max, Myc and Mad at various temperatures to determine the equilibrium dissociation constants and ΔH^o, ΔS^o, and ΔG^o of Max_2, Myc-Max and Mad-Max dimmers using equation *6*.

Studies in Section 1.5 showed that binding of Max monomer to E-box DNA significantly reduced the binding of the second monomer, whether the monomer was Max, Myc, or Mad. Other studies (30) have shown that dimerization rates of bz and b/HLH/z proteins increase in the

presence of negatively charged polymers including specific and nonspecific DNA, presumably through charge neutralization. In order to further understand the effects of DNA on the dimerization and the protein-protein interactions, the effect of polyions on dimer formation were examined.

1.6a Results:

Myc, Max and Mad are relatively unstructured as monomers. Their α helices are properly folded only when their dimerization interfaces are properly aligned whether or not they are bound to DNA. Kohler et al 1999 (1) have shown by CD measurements that at low concentration (25-100 μM range) Max is largely unstructured and therefore presumed to be in a monomeric state. Similar experiments (data not shown) in our laboratory confirm this observation. Thus in order to determine monomer-dimer dissociation constants, TRITC labeled Max at 50 nM concentration was titrated with unlabeled Max, Myc or Mad. Thermodynamic parameters were obtained from the temperature dependence.

Figure 15 shows the binding of unlabeled Max to Max-TRITC as a function of temperature. The observed anisotropy change r_{obs} of Max-TRITC was plotted vs concentration of unlabeled Max. The data were fitted to Equation 5 and K_ds were determined. The lines indicate the fitted curves. Similar sets of data were obtained for Myc (Figure 16) and Mad (Figure 17) titrations with labeled Max-TRITC. The temperature dependence of the reactions were plotted (Figure 18) and used to determine ΔG°, ΔH° and ΔS° according to Equation 6. Table 6 shows the K_ds, enthalpy and entropy of dimerization of Max_2, Myc-Max and Mad-Max. Comparison of the individual dissociation constants indicate that at 33° C, which is close to physiological temperature, the binding of Myc to Max is about 2.5 and 1.4 times higher affinity than binding of Max_2 and Mad-Max, respectively. The association of all three dimers becomes even stronger at lower

temperature. However, the differences in association between Max_2 and Mad-Max becomes less. These trends are reflected in the thermodynamic parameters. All three dimerizations are enthalpically favored and entropically unfavorable. Table 7 shows the calculated ΔG° values. Interestingly, the ΔG° values at 37 ^{0}C are the same within experimental error for Myc and Mad associating with Max and only slightly less favorable for Max homodimer formation. The unfavorable entropy is compensated by the favorable enthalpy. Mad has a significantly lower entropic contribution compared to Myc or Max.

Studies in section 1.3 and 1.5 showed the importance of E-box DNA on the protein-protein binding affinity. Looked at from the perspective of the Max protein, DNA binding reduced binding of the second monomer regardless of whether the monomer was Myc, Mad or Max. In order to further investigate whether DNA itself was responsible for the lower bindng of the second monomer or if charge neutralization was sufficient, the effects of polyions were investigated. Kohler et al. (31) have shown that proteins that use the monomeric pathway for DNA binding and dimerization are able to form dimers at a higher rate in the presence of negatively charged polymers. These polymers essentially substitute for DNA (20). Negatively charged polymers can neutralize the charge on the basic contact regions of the proteins and bring the dimers together more easily. Rentzeperis et al. (32) have shown that in case of Arc repressor, refolding of the protein into a functional dimer is accelerated in the presence of polyanions.

The effects of both positive and negative polyions on the equilibrium binding of Max, Myc and Mad to TRITC labeled Max were investigated. Positively charged poly-L-lysine showed little effect on the K_d of c-Max, Mad-Max and Max_2 dimers (data not shown). However, poly-L-glutamic acid, PLG, significantly reduced the K_ds for all three protein dimers. There were marked differences in the thermodynamic parameters for all three protein complexes. Figures 19, 20 and 21 show the effects of PLG on Max homodimer, Myc-Max, and Mad-Max formation,

respectively. Table 8 lists the K_ds calculated from the plots and the thermodynamic parameters calculated from the temperature dependence (Figure 22). One important observation is that although the protein-protein interactions in the presence of PLG become tighter for all three dimers, the difference in binding affinity between Myc-Max, Mad-Max and Max-Max remains in the same order as in absence of PLG (Myc-Max K_d is 2.4 times Max-Max and 1.28 times Max-Mad). Table 8 shows that the enthalpy and entropy for each dimer is more negative in the presence of PLG. PLG enhances the stability of all three dimers by 2-3 kJ/mol (Table 9).

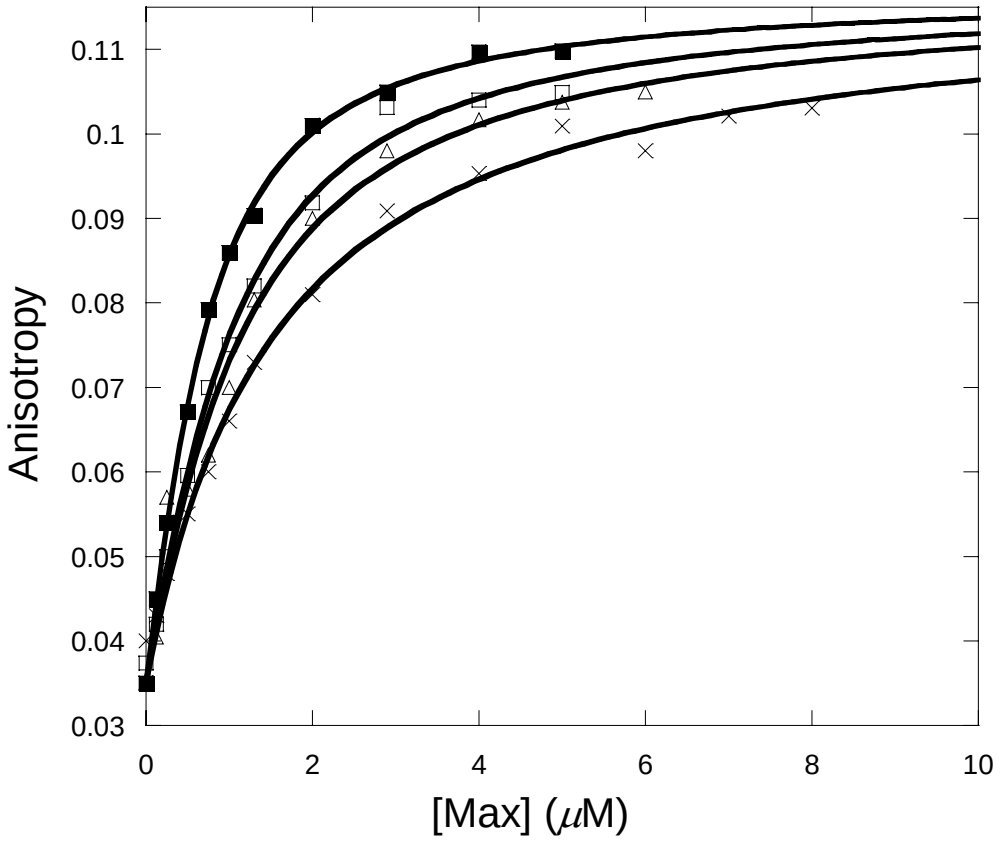

Figure 15: Titration of 50 nM Max-TRITC (Excitation at 540 nm and Emission at 576 nm) with unlabeled Max at 13 °C (■), 23 °C (□), 28 °C (Δ) and 33 °C (×) in pH 7.6 HEPES-KOH buffer (as described in section 1.3).

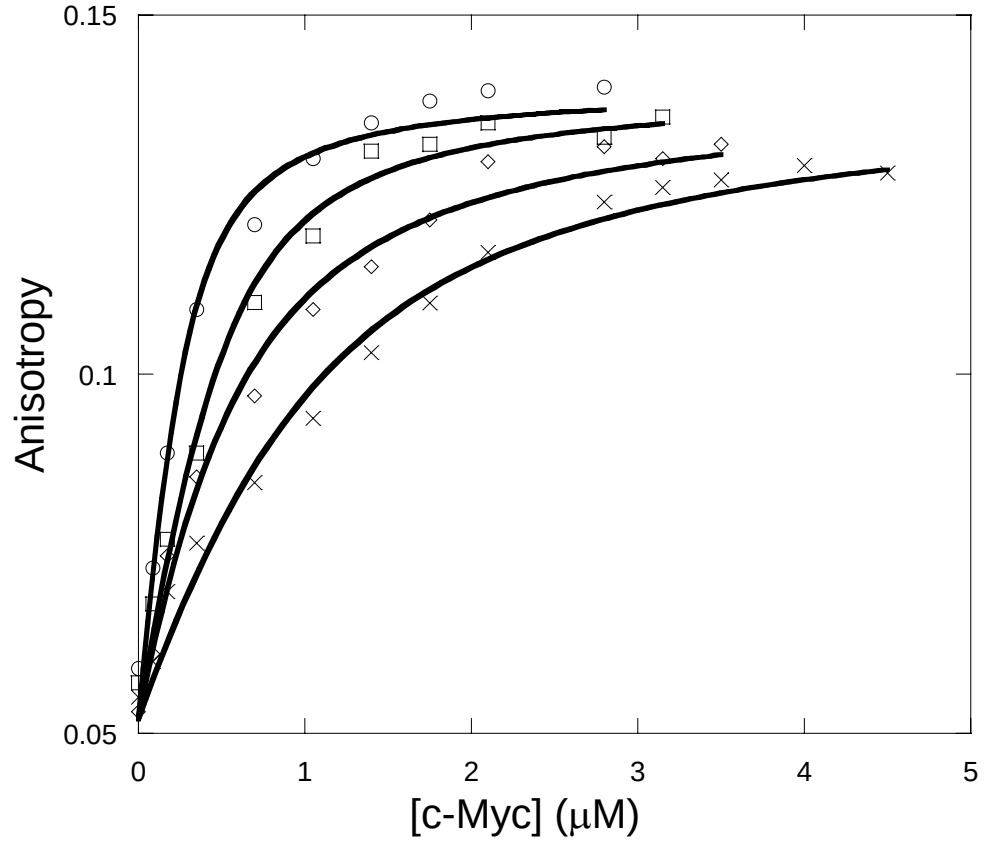

Figure 16 Titration of 50 nM Max-TRITC with unlabeled c-Myc at 13 °C (◊), 23 °C (○), 28 °C (×) and 33 °C (□). Experimental conditions are as described in Figure 15.

.

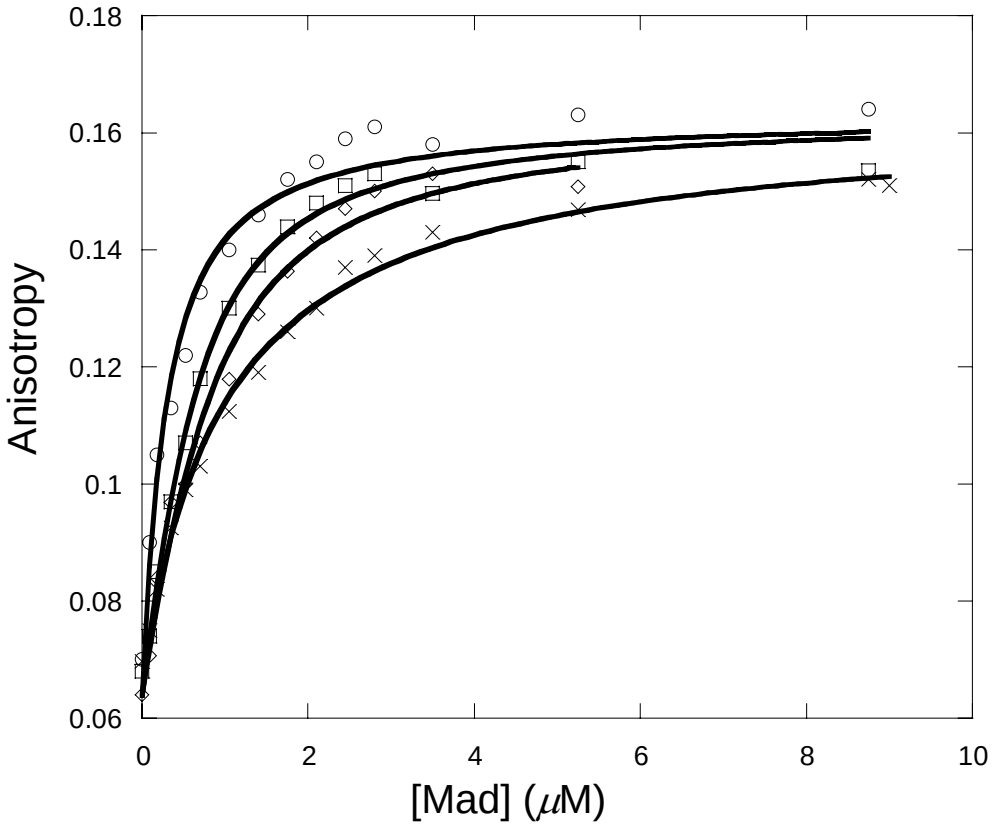

Figure 17 Titration of 50 nM Max-TRITC with unlabeled Mad at 13 °C (○), 23 °C (□), 28 °C (◊) and 33 °C (×). Experimental conditions are as described in Figure 15.

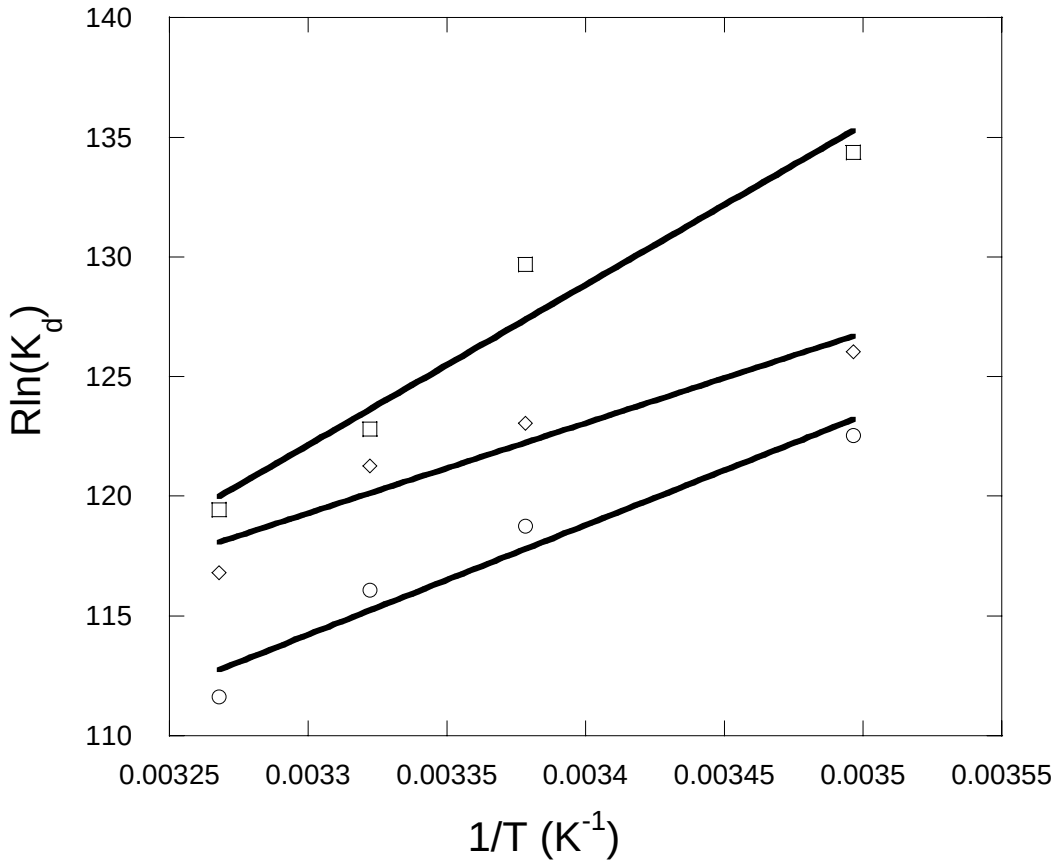

Figure 18 vant Hoff's plot for titration of 50 nM Max-TRITC with c-Myc (□), Max (○) and Mad (◊). K_d values are from data in Figures 15, 16 and 17.

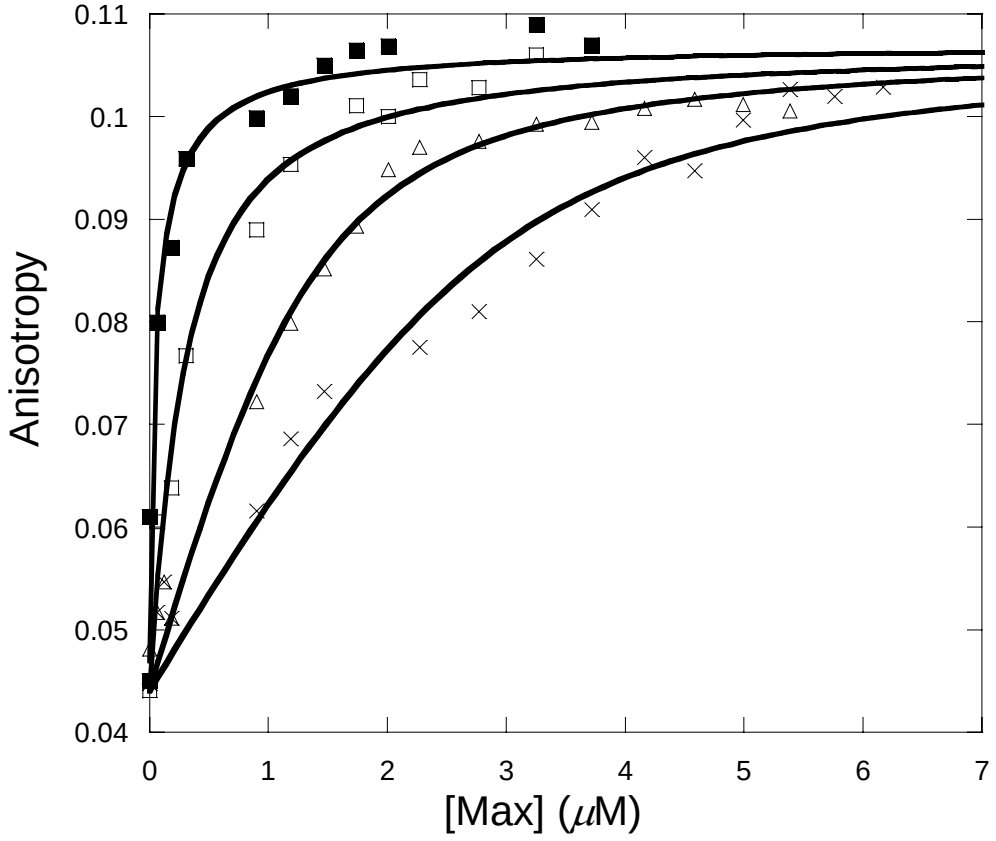

Figure 19 Titration of 50 nM Max-TRITC with unlabeled Max in presence of 150 μM Poly-L-Glutamic acid at 13 ºC (■), 23 ºC (□), 28 ºC (Δ) and 33 ºC (×). Experimental conditions are as described in Figure 15.

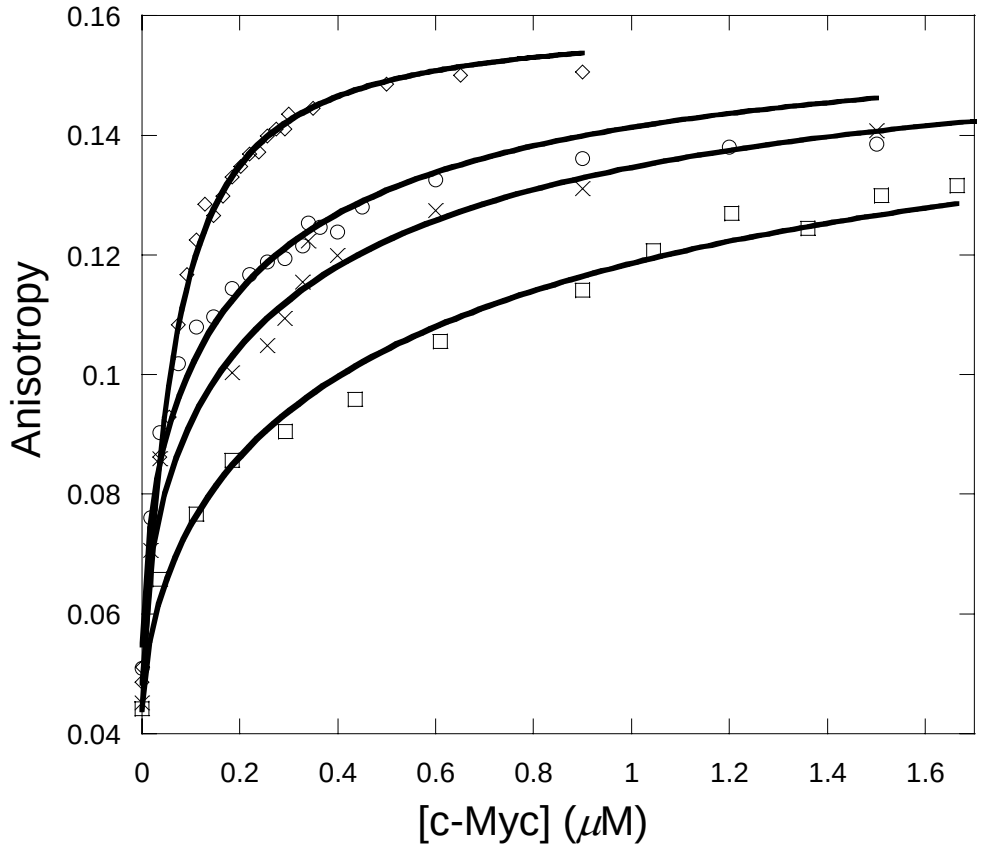

Figure 20 Titration of 50 nM Max-TRITC with unlabeled cMyc in presence of 150 μM poly-L-Glutamic acid at 13 ºC (○), 23 ºC (□), 28 ºC (◊) and 33 ºC (×). Experimental conditions are as described in Figure 15.

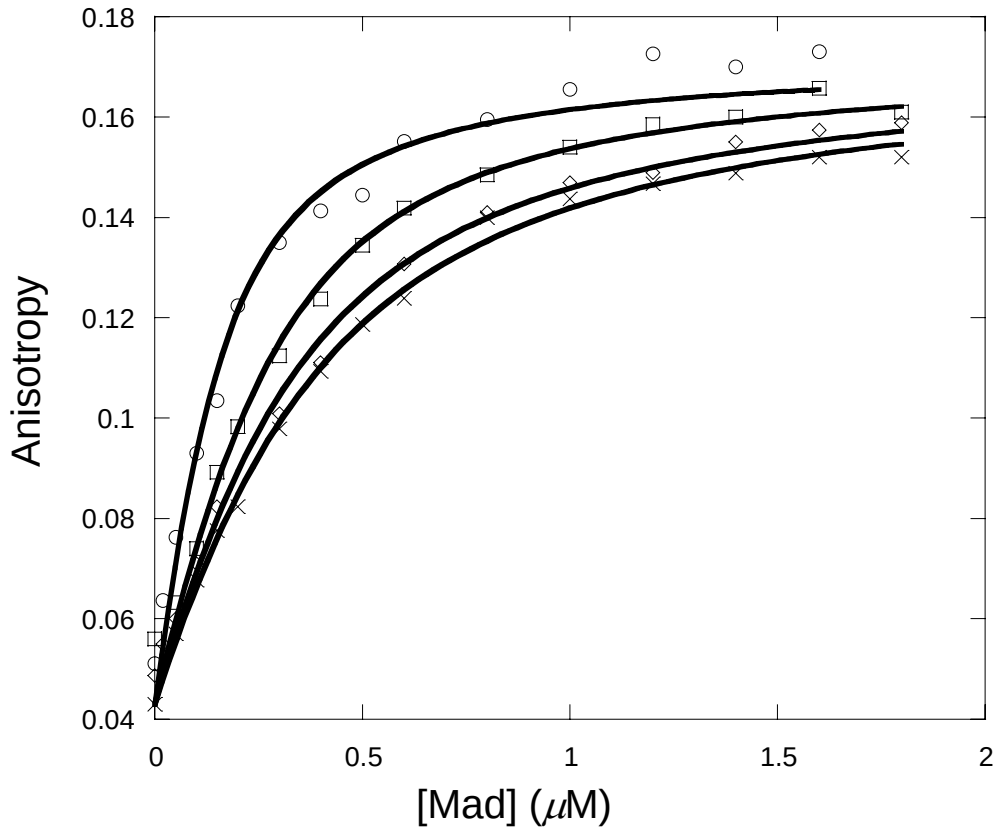

Figure 21 Titration of 50 nM Max-TRITC with unlabeled Mad in presence of 150 μM poly-L-Glutamic acid at 13 °C (○), 23 °C (□), 28 °C (◊) and 33 °C (×). Experimental conditions are as described in Figure 15.

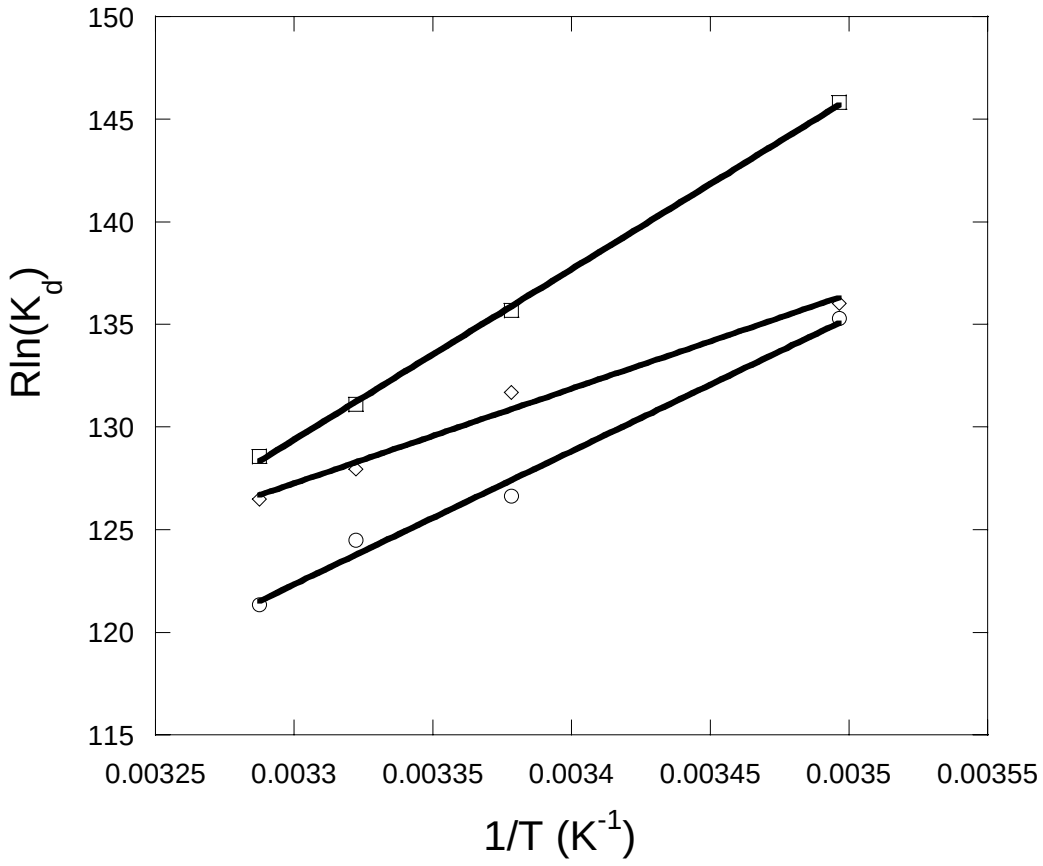

Figure 22 van't Hoff plot for titration of 50 nM Max-TRITC in presence of 150 μM Poly-L-Glutamic acid with c-Myc (□), Max (○) and Mad (◊). K_d values were obtained from Figures 19, 20, and 21.

.

	K_d (μM) at 13 ºC	K_d (μM) at 23 ºC	K_d (μM) at 28 ºC	K_d (μM) at 33 ºC	Δ Hº (kJ/mol)	ΔSº (J/mol)
Max	0.392±0.02	0.622±0.06	0.857±0.16	1.47±0.14	-45.7±7.6	-36.8±15.5
c-Myc	0.095±0.02	0.167±0.03	0.382±0.05	0.573±0.09	-66.8±1.1	-98.6±17.4
Mad	0.259±0.04	0.371±0.03	0.460±0.07	0.786±0.09	-37.6±8.3	-4.9±10

Table 6. Thermodynamic parameters for association of Max, c-Myc, and Mad with Max-TRITC

	Δ Gº (kJ/mol) at 10 ºC	Δ Gº (kJ/mol) at 20 ºC	Δ Gº (kJ/mol) at 37 ºC
Max	-35.3	-34.9	-34.3
c-Myc	-38.9	-37.9	-36.2
Mad	-36.2	-36.2	-36.1

Table 7. ΔG^0 values calculated from Table 6 and Equation 6.

	K_d (μM) at 13 ºC	K_d (μM) at 23 ºC	K_d (μM) at 28 ºC	K_d (μM) at 33 ºC	Δ Hº (kJ/mol)	ΔSº (J/mol)
Max	0.085±0.01	0.241±0.05	0.312±0.06	0.455±0.15	-64.9±4.8	-91.8±16.4
c-Myc	0.024±0.09	0.081±0.05	0.141±0.02	0.191±0.05	-83.0±1.4	-144.7±5.0
Mad	0.078±0.01	0.131±0.02	0.206±0.02	0.245±0.01	-46.1±4.3	-24.8±14.5

Table 8 Thermodynamic parameters for association of Max, c-Myc and Mad with Max-TRITC in the presence of 150 μM poly L-glutamic acid.

	Δ Gº (kJ/mol) at 10 ºC	Δ Gº (kJ/mol) at 20 ºC	Δ Gº (kJ/mol) at 37 ºC
Max	-38.9	-38.0	-36.4
c-Myc	-42.1	-40.6	-38.2
Mad	-39.1	-38.8	-38.4

Table 9. ΔG^0 values calculated from Table 8 and Equation 6.

1.7 Binding Study of inhibitor compounds to Myc-Max and Mad–Max heterodimers by Fluorescence anisotropy

Myc has strong oncogenic potential and its dimerization with Max is an absolute necessity for exerting such effects (2). These, requirements for dimerization may allow control of Myc activity with small molecules that interfere with Myc-Max dimerization.

Berg et al. (33) screened one such combinatorial peptidomimetic library created by Boger et al. (34) and identified two such candidate compounds which inhibited Myc-Max dimerization and also their DNA binding.

In order to investigate the mechanism of binding of these inhibitors to Myc/Max proteins we used fluorescence anisotropy of TRITC labeled Max, followed by titration with unlabeled Myc in the presence of the most potent inhibitor IIA6B17 (fig 23) and also compared the result with the control compound IIA4B6. To further study, if this inhibition of Myc-Max dimerization by Berg et al. (33) was Myc specific we repeated the same experiment with TRITC labeled Max and unlabeled Mad. The experimental details are as follows:

IIA6B17 and IIA4B6 were dissolved in 8% DMSO and added to 25 mM HEPES-KOH buffer, pH 7.6 containing 50 nM Max-TRITC, in 25, 100, 200 μM concentration and titrated with unlabeled Max, Myc or Mad until the anisotropy value reached saturation. Protein purification and labeling of Max was according to Sections 2.1a and 2.1b.

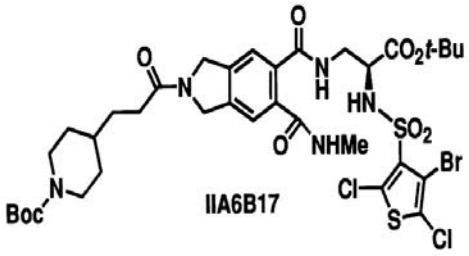

Figure 23 Active Inhibitor

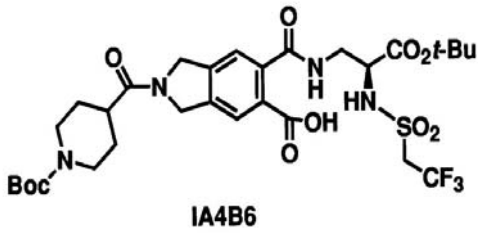

Figure 24 Negative Control

A Lineweaver-Burk plot of 1/Δr vs 1/[Myc] or [Mad] was plotted, Figure 25. K_I (the equlibrium constant for binding of the inhibitors to the proteins) was calculated from the following equation:

$(1+[I]/ K_I)*[S]/r_{max}$= slope *(10)*

Where r_{max} is the maximum anisotropy obtained in each set of titration and [S] is the concentration of Myc or Mad at $r_{max}/2$. [I] is the concentration of the inhibitor used.

1.7a Result:

Reciprocal of the anisotropy 1/Δr when plotted vs. reciprocal of [Myc] in presence of different concentrations of the inhibitor resulted in a plot, which is consistent with competitive inhibition (Figure 25). When the same experiment was repeated for Mad-Max dimerization, it was observed that binding of Mad to Max was also competitively inhibited by IIA6B17 competitively (fig 26). The K_I s were calculated (Table 10) according to equation 9. Iinhibition of dimerization of Myc or Mad to Max by the inhibitor is in the same range, the effect being slightly stronger in case of Mad-Max. The control compound IIA4B6 had no significant effect on dimerization of either Myc or Mad. We also tried the same experiment with TRITC labeled Max titrated with unlabeled Max in the presence of inhibitors. This gave rise to very unstable anisotropy changes, hence the data were not plotted.

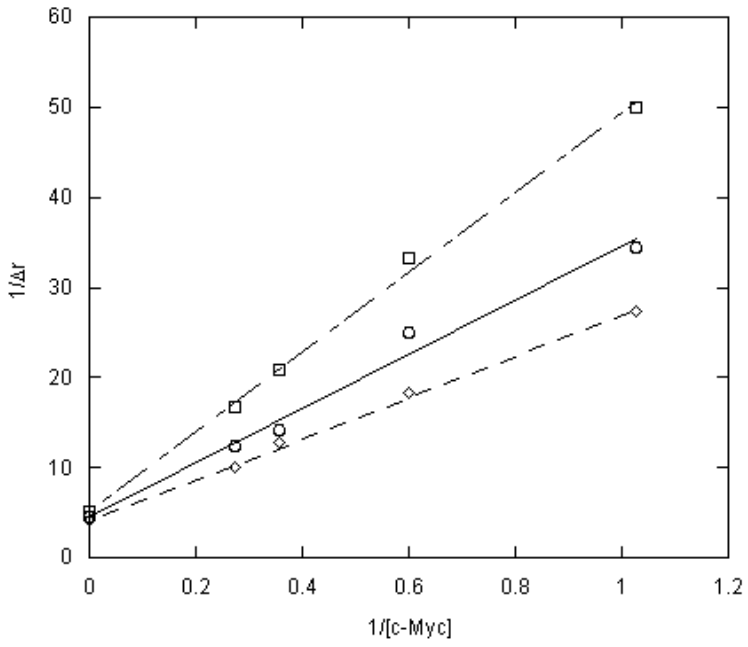

Figure 25:Lineweaver-Burk Plot of Titration of 50 nM Max-TRITC (Excitation 540 nm and Emission 576 nm) in presence of 25 μM (x), 100 μM (○) and 200 μM (□) inhibitor IIA6B17 with c-Myc 23 °C. Experiments were performed in 25 mM HEPES-KOH buffer pH 7.6.

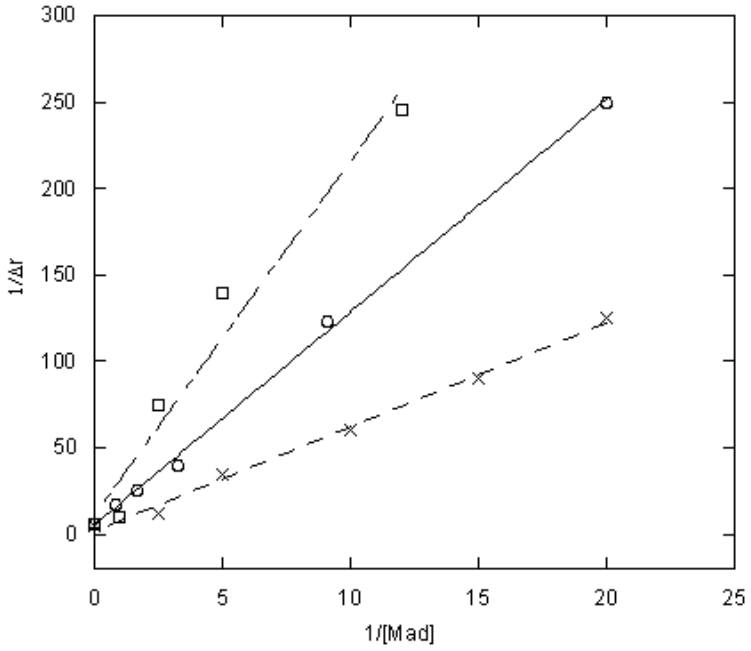

Figure 26: Lineweaver-Burk Plot of Titration of 50 nM Max-TRITC in presence of 25 μM (x), 100 μM (○) and 200 μM (□) of inhibitor IIA6B17 with Mad. Experimental conditions are as described in Figure 26.

Max-TRITC +	K_I in presence of IIA6B17 (μM)
c-Myc	77.8±8.2
Mad	57.1±2.3

Table 10: K_I calculated from Equation 9 using data from Figures 25 and 26, Compound IIA6B17 was a competitive inhibitor of Myc-Max and Mad-Max dimerization.

1.8 Discussion:

The Max-DNA binding profiles indicated Max dimer binding to DNA and did not show a biphasic binding mode which has been observed with USF (27).Our study of DNA-protein interactions show that there is a significant difference on the behavior of heterodimers interacting with DNA compared to Max homodimer binding DNA. The Max protein binds DNA with higher affinity, while Myc or Mad contributes more towards specificity of DNA recognition. These results also support some previous studies on the binding preference that Myc-Max heterodimers binding only a subset of the sites bound by Max homodimer, possibly due to a differential recognition of the DNA flanking sequences (24)**.**

When protein-protein interaction was determined by fluorescence anisotropy of labeled Max, the anisotropy signals for the protein dimerization reflected the difference in molecular size for these three dimers. The Max dimer is similar in size to Myc-Max dimer, but the Mad-Max is much larger. In contrast to Nair et al.'s suggestion (19) that a tetramer formed for Myc-Mac, there is no evidence to show the formation of tetramer at the protein concentration in our experimental system. We suggest here that the formation of tetramer might only occur in higher concentrations but not at physiological conditions. Cross-linking of the Max protein (19) might affect the protein-protein interaction.

The protein-binding pathway was studied by to measuring the equilibrium constants for all of the interaction steps shown in Figure 13. The monomer-DNA binding measurement was limited due to the small changes of the mean hydrodynamic volume V_h with or without DNA oligos (if protein is labeled and titration is performed by adding DNA) and the monomer-DNA, dimer-DNA interaction occuring (if DNA is labeled and titration is performed by adding more protein). Instead of detecting this interaction in a Max only system, two heterodimer DNA systems were

used to approach this problem. In this heterodimer-binding assay, K_1, K_3 and K_4 were obtained directly from a series of the titration experiments and thus K_2 was calculated from the relationship (Figure 13):

$K_1 * K_4 = K_2 * K_5$

Recently Park et al. (35) determined the kinetic rate constants for Myc-Max and Max-Max binding to an E-box oligonucleotide by gel electrophoresis. From the kinetic data, they obtained equilibrium constants for dimer binding to DNA and monomer-dimer equilibria. Equilibrium constants for dimer binding were similar to our results for Myc-Max binding to DNA (K_{eq} = 145 nM, our data 90.5 nM). The data presented here, however, for Max dimer binding, show an almost 7-fold tighter binding to DNA compared to the values obtained by Park et al. Similarly Park et al. show lower monomer-dimer affinity for Myc-Max interaction (78 μM compared to 176 nM). The differences in monomer-dimer equlibria may result from slightly different experimental conditions or from the difficulty in obtaining monomer-dimer values from gel electrophoresis experiments.

Based on the equilibrium values obtained, the *in vitro* pathway during a titration follows a monomer pathway, which is consistent with kinetic data (1). The binding of Max monomer occurs at concentrations well below the formation of dimers. The pathway forms a thermodynamic cycle and therefore the stability of the final complex will not depend on the pathway followed. These equilibrium data suggest that at physiological conditions, most of the DNA would have Max homodimer bound. Displacement and binding of the second (different) monomer to form a heterodimer-DNA complex may serve to aid in selection of DNA. The heterodimer binding affinity to non-E-box DNA is much lower. Therefore, if Max_2-DNA is bound to a less favorable site, the displacement by Myc or Mad may well cause release of the protein. However, it is interesting to observe that the second monomer has much lower affinity

for the monomer-DNA than the first monomer binding to DNA (micromolar compared to nanomolar affinity). It is clear from these data that binding of DNA to the Max monomer reduces the affinity for the second monomer. Looked at from the perspective of the Max protein, DNA binding reduces the affinity of Max for its partner protein. This is true whether Max forms heterodimers with Myc or Mad or forms a homodimer with a second Max monomer. Comparing K_2 with K_4, the second monomer is destabilized by 6.2 and 6.8 kJ/mole for Myc-Max or Mad-Max, respectively. These results are somewhat surprising given the stability of the dimer-DNA complex. The destabilization or anticooperative binding may result from the conformational change that monomers are believed to undergo upon binding. The basic region is largely unstructured in solution, but folds to an alpha helix upon binding to DNA. Whether this change occurs on the monomer level or only after the dimer has formed has not been determined. The effects of this conformational change on equilibria may be to destabilize non-specific interactions. The monomers are believed to have a fast on and off rate. A second monomer association may induce the conformational change, which results in a more rigid conformation that interacts more precisely with the E-box. This dimer may have slower on and off rates. The equilibria predict that the binding of the second monomer reduces the site occupancy, but the kinetics may determine the rate of formation of the complex. Another result of weak binding of the second monomer could be to facilitate reassortment of the partners of Max, switching from transcription activation to repression.

The data reported here give new insight into the assembly of protein-DNA scaffolding and support the importance of protein-protein interactions in determining the selection and stability of dimer-DNA complexes. Further interactions of other protein factors such as Mnt and Mxl are likely to alter the stability of these complexes, largely through the protein-protein interactions.

Such changes in stability are predicted to be important in regulation of the transcription complex composition and function and are possible targets for therapeutic intervention.

For defining protein-protein interactions, formation of more stable heterodimers could be explained in terms of specific amino acid interactions as observed in the crystal structure of Myc-Max, Mad-Max and Max-Max (20). The three dimensional structures of Max homodimer and Max-Myc and Max-Mad heterodimers reveal hydrophobic interactions along the extensive protein-protein interface (buried solvent accessible area) in addition to hydrogen bonding in the periphery of the leucine zipper that may be responsible for stability and specificity of dimerization (19, 20).

In Max homodimer, a tetrad association occurs between Gln91-Asn92-Gln91-Asn92 with Gln91 of one LZ at position g and Asn 92 at position a of the other LZ. This creates a packing defect in the homodimer interface. However in Myc-Max heterodimer, Gln91 and Asn92 in Max can form stronger H bonding with positively charged Arg423 and 424 in Myc resulting in closer protein-protein interactions. A similar situation arises in the case of Mad-Max where a Glu125 hydrogen bonds with Asn92 in Max.

In an NMR study with vMyc, Bister et al. (36) demonstrated that the b/HLH/z domain of vMyc was pre-structured in solution with two α helical subdomains. The presence of such a well ordered structure may also occur in c-Myc and might serve as the nucleus for specific association with Max. Negative entropy changes are generally associated with loss of rotational and translational degrees of freedom (37). Bister et al (36) have argued that in the case of vMyc, the presence of preformed secondary structure might restrict the conformational mobility of the protein. In our study, the highest negative unfavorable entropy was found for the Myc-Max dimer. This suggests that the pre-formed structure of Myc can influence significantly the association with other proteins.

Further, the data reveal that among the three protein dimers, Mad-Max probably has the most conformational flexibility, which could account for its relatively less negative (-4.9 kJ/mole) entropy of dimerization. It will be interesting to see if NMR or other solution studies can confirm this prediction.

The low stability of the Max homodimer permits reassortment with monomers of its interacting partners and this destabilization of the homodimer can serve as a prominent driving force for efficient heterodimerization (20).

Our data for protein-protein interactions in presence of PLG shows that interaction becomes tighter in case of all three dimers in presence of negative polyions.

Negative enthalpy and entropy are characteristic of involvement of van der Waals forces and hydrogen bonding in protein-protein interactions (37). Crystal structures and NMR studies have revealed the importance of hydrogen bonding between charged and uncharged polar residues in these protein dimers. It has also hypothesized by Ross et al (37) that hydrogen bond formation in a low dielectric environment is an important source of negative enthalpy and entropy. Mobile polyanions like PLG can create a low dielectric environment by shielding positive charges on the protein-protein interacting interfaces, which is a possible reason for the more negative ΔH° and ΔS° for Myc-Max, Mad-Max, and Max-Max association in the presence of PLG. As monomers, the individual protein subunits exist in full or partial unfolded form. Such unstructured or partially structured monomers can nonspecifically collide on the surface of the polyanions more rapidly through electrostatic interactions. These collisions appear to be more productive for proper folding and stronger association of the monomers. Dimerization on the DNA surface occurs through a similar mechanism. From our results, it can be concluded that the presence of negatively charged DNA and RNA in the cell nucleus at high concentration or changes in the environment such as histone deactylation, protein phosphorylation or other events can

nonspecifically help in dimerization of Myc-Max, Mad-Max and Max_2 dimers. Further, the significant differences in entropy for formation of Myc-Max and Mad-Max heterodimers suggests that small molecules that restrict the conformational flexibility could selectively affect heterodimer formation and possibly biological function.

Berg et al (33) demonstrated that IIA6B17 is a potential inhibitor of Myc-Max dimerization, and could result in reduction of oncogenic transformation. The docking target of the inhibitors, or mechanism of such inhibitions was not elucidated. The initial experiments with these inhibitors in our laboratory suggest that these compounds competitively binds to the HLH/z domain of these proteins, since both Myc-Max and Mad-Max dimerization were inhibited. Moreover our experiments clearly demonstrate that these inhibitors also effect Max homo dimerization. Hence small molecules which can specifically target only Myc or can stabilize Max homodimerization, resulting in less availability of Myc for transcription activation could be ideal as therapeutic targets of tumorigenesis caused by Myc.

Chapter 2

2.0 DNA conformational change induced by binding of Max_2, Myc-Max and Mad-Max heterodimers: A Fluorescence Resonance Energy Transfer Study.

The regulation of transcription initiation in eukaryotic organisms depends on asssembly of protein-DNA molecular surfaces in the correct orientation as well as changes in conformation of these complementary molecular species. As a prerequisite or a consequence of such interaction, DNA conformation can be either actively modified locally by proteins, or it can passively adopt an altered conformation as a result of looping mediated by proteins that bind to separate recognition elements (1).

An interesting finding on interactions among transcription factors that bind to separate sequence elements has been that this kind of association requires bending of the intervening DNA (2,3). DNA bending in recent years has also been an important field of research due to the fact that it is important for chromatin remodeling. Therapeutic effects of certain drugs are based on their ability to recognize bends in their target DNA sequences. For example, the anticancer activity of certain drugs such as Cisplatin arises from their ability to damage DNA, with the major adducts formed being intrastrand d(GpG) and d(ApG) crosslinks. These crosslinks bend and unwind the duplex, and the altered structure attracts high-mobility-group domain (HMG) and other proteins (4). Many HMG-domain proteins recognize altered DNA structures such as four-way junctions (3, 5).

Reports have also confirmed for drugs that are regarded as TOP1 poisons, a DNA bending sequence can substitute for the drug-DNA complex in stimulating topoisomerase I-mediated DNA cleavage. In such instances it is possible that the drug stimulates topoisomerase I-mediated DNA cleavage by inducing a bend in the DNA within the ternary complex (6).

DNA bending in chromatin structure modification is also important. Experiments with many DNA binding proteins have demonstrated a strong correlation between the ability to bend DNA and nucleosome sliding, suggesting that the sliding is induced by the bend (30). Nucleosomal sliding during chromatin remodeling is important for controlling gene expression (28).

Phasing analysis, a method that is based on the phase-dependent interaction between two closely spaced bends in DNA has revealed a simple and elegant mechanism for cooperative DNA recognition by the b/HLH/z protein families (2, 7). Fos–Jun heterodimers and Jun homodimers induce DNA bending in opposite directions (2, 5). However, x-ray crystallographic analysis of peptides encompassing the minimal basic DNA binding and leucine zipper dimerization domains of Fos and Jun bound to the AP-1 site detected little DNA bending (6). Investigation by Crothers et al. using gel-based methods have also failed to detect substantial DNA curvature induced by protein binding (5). Thus, additional methods are required for analysis of the structural basis of protein-induced DNA bending.

By taking advantage of the altered mobility of protein-bound DNA in the mobility shift assay, at least two laboratories in the early 1990s demonstrated that homo- and heterodimeric complexes of c-Myc and Max are able to cause increased DNA flexure as measured by the circular permutation assay. According to their observations, c-Myc and Max homodimers bend DNA in opposite orientations, whereas c-Myc-Max heterodimers cause a smaller bend, in an orientation similar to that induced by Max homodimers (7, 8).

However, the recently published x-ray structure of Myc-Max and Mad-Max as well as that of Max homodimers by Burley et al (9, 10) do not display comparable evidence of DNA bends. A more recent study employing circularization kinetics (11) and affinity measurements studies with prebent DNA templates for assessing bending and DNA structural preferences for Max and other

b/HLH/z proteins failed to detect any bent DNA in solution. It was rather concluded that Myc/Max- b/HLH/z family of proteins actually stabilize DNA in an unbent configuration that resists circularization. The anomaly in mobility was found to be induced by the leucine zipper motif, rather than structural distortions of DNA. The study suggested that rigid protein domain structures may induce anomalous electrophoretic mobility which could be misinterpreted to be a consequence of DNA bending induced by the protein (11).

Hence whether or not these homodimers and heterodimers induce DNA bending is still open to debate. We used a FRET based method to identify if Myc-Max-Mad protein complexes can induce bending of the cognate DNA.

2.1 Material and Methods:

c-Myc, Max and Mad proteins were purified as described by Hu et al. (31). Double labeled, single labeled and unlabeled oligonucleotides (Table 11) were purchased from Gene Link Inc (Hawthorne, NY 10532) and Integrated DNA Technology (Coralville, IA 52241). Complementary oligonucleotides were annealed in nuclease free water purchased from Promega, (Madison WI 53711) heated at 85-90 °C for 30 minutes and then cooled to room temperature over a period of 12 hrs-overnight.

Oligonucleotides with their names and modifications are presented below:

Table 11: Oligonucleotides used in FRET study

MLP1 : **ROX** -5’ CCCG*GTGCAC*TGGC‘3-**Fluorescein**

GGGC*CACGTG*ACCG

MLP2 : 5’GGGC*CACGTG*ACCGC-**TAMRA**

Fluorescein -3’CCCG*GTGCAC*TGGCG

MLP14’3: 5’CCCG*GTGCAC*TGGC‘3-**Fluorescein**

GGGC*CACGTG*ACCG

MLP14: **5’CCCG***GTGCAC*T**GGC‘3**

GGGC*CACGTG*ACCG

A TRACT: 5’AAAACACGTGAAAA’3-**TAMRA**

Fluorescein –3’TTTTGTGCACTTTT

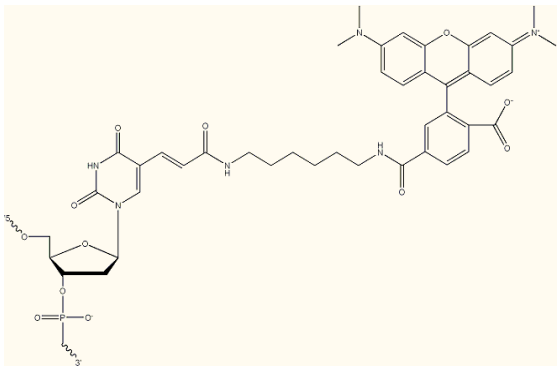

Figure 27 TAMRA (Carboxy tetramethyl Rhodamine) attached to DNA terminus

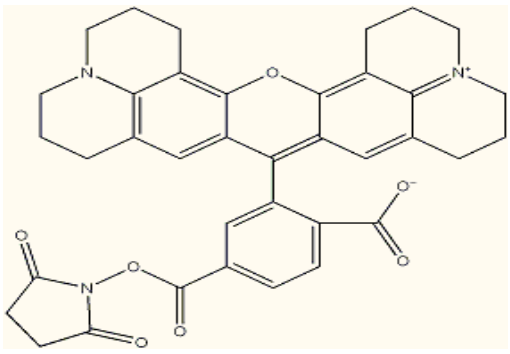

Figure 28 ROX (Carboxy-X Rhodamine)

2.1b FRET Experiment:

The FRET efficiencies were determined by measuring the intensity of the sensitized emission of the acceptor normalized to the fluorescence of the acceptor alone using equation (3). $Ratio_A$, the fitted weighting factor of the two spectral components is linearly dependent on the efficiency of energy transfer E. $Ratio_A$ normalizes the measured sensitized FRET signal for concentration, quantum yield of acceptor and for any errors in the percentage of acceptor labeling (12, 13).

$(ratio)_A$ is calculated from equation *(11)* by the following method (shown for measurement of MLP1): An integrated emission spectrum of MLP14'3, from 500 to 530 nm, labeled with donor dye fluorescein only (excited at 480 nm for MLP1 and 490 nm for MLP2) is subtracted from the integrated spectrum (500-610nm for MLP1 and 500-580 for MLP2) of the donor acceptor labeled DNA i.e.MLP1 or MLP2. The resulting spectrum consisting of only emission spectrum of ROX or TAMRA is divided by an integrated spectrum (550-610nm for MLP1 and 530-580 for MLP2) of the same donor, acceptor labeled molecules. F^{DA} is the fluorescence of donor-acceptor labeled DNA and F^{D} is the fluorescence of only donor labeled DNA. $[\lambda]_{em}$,480 or $[\lambda'']_{em}$,560 are the excitation wavelength at which the donor-acceptor or only donor labeled DNAs are excited. Energy transfer efficiency E can then be calculated by equation *12* (shown for measurement of MLP1 only).

$$(ratio)_A = [\sum F^{DA}([\lambda]_{em},480) - \sum F^{D}([\lambda]_{em},480)]/ \sum F^{DA}([\lambda'']_{em},560) \quad (11)$$

$$E = \{(ratio)_A) - ([\varepsilon]^{A,480}/[\varepsilon]^{A,560}) * ([\varepsilon]^{A,560/}[\varepsilon]^{D,480}) \quad (12)$$

. In equation *12* ε^D and ε^A are the molar absorption coefficients at the indicated frequency of donor and acceptor, respectively and are measured from absorption spectra (13).

Binding of Max_2, Max-Myc and Max-Mad to labeled DNAs were verified by monitoring the anisotropy of the fluorescein emission at 518-520 nm vs protein concentration and dissociation constant K_{ds} were calculated using Equation 5 (16).

The equilibrium dissociation constant for the Max dimer-DNA interaction was also determined by monitoring the decrease in fluorescein emission at 520 nm as a function of Max concentration. The concentration of DNA was fixed at 50 nM, and the concentration of Max was varied. The data were fit to eq *13* (16).

$$F_{obs} = F_{max} - \{(F_{max} - F_{min})/(2*[DNA]_{tot}) * \{b - (b^2 - 4[Max]_{tot}[DNA]_{tot})^{1/2}\} \qquad (13)$$

Where $b = K_d + [DNA]_{tot} + [Max]_{tot}$

where F_{obs} is the observed fluorescence for any mixture of Max and MLP1 or MLP2 and F_{max} and F_{min} are the maximum and minimum fluorescence intensities in free donor-acceptor labeled DNA and Max bound saturated state of the same DNA respectively, monitored during FRET experiment..

Fluorescence resonance energy transfer studies were performed with a Spex Tau 2 Fluorolog Spectrophotometer from Spex, Edison, NJ, with excitation and emission slits at 3mm and 5mm respectively. 50nM DNA in HEPES Buffer pH. 7.6 (20 mM KCL, 0.5 mM $MgCl_2$, 0.5mM EDTA, 1mM DTT) was titrated with Max homodimers or preformed Myc-Max and Mad-Max heterodimers until saturation. Myc-Max and Mad-Max heterodimers were formed by adding excess Myc and Mad to Max in pH 7.6 HEPES buffer to allow complete heterodimerization. Scans were measured from 500-650 nm at excitation 480 for MLP1 and 500-600 nm with excitation at 490 for MLP2. All the energy transfer data were calculated using equation *(2)*, *(3)* and *(11)* and *(12).*

2.2: Result

To investigate the extent to which DNA conformation is changed due to binding of Max_2, Max-Myc or Max-Mad dimer complexes, MLP1 and MLP2 (table 11) were titrated with Max homodimer and Myc-Max and Mad-Max heterodimer.

In order to confirm that binding affinities of the protein complexes with MLP1 and MLP2 DNA are not affected due to labeling of either ends of DNA, 50 nM of such DNA oligos were titrated with three different protein dimers and anisotropy of the fluorescein peak was observed at 520 nm (Figure 29). Dissociation constants K_{DS} (Table 12), calculated from the curves in Figure 29 for MLP1 oligo, using equation 5 (15) agreed with our earlier K_{ds} calculated from only FITC labeled DNA (29).

When MLP1 was titrated with Max and the entire range from 500 to 650 nm of the fluorescence emission spectrum was scanned, a substantial decrease of the donor fluorescein peak at 520 and increase of the acceptor ROX peak at 607 nm was observed. The decrease in fluorescein peak at 520 plotted vs concentration of Max, (Figure 30) could also be used to calculate the dissociation constant (Table 12) for Max-DNA binding using equation 13. The dissociation constants, K_d, obtained by anisotropy measurement, 14.1±2.4 nM compared to 28.9±5.8 nM by FRET are within an acceptable range considering the two different methods used to obtain K_d.

Decrease of the donor fluorescence at 520 (Figure 30) and the increase of the acceptor peak at 607 (Figure 31) of MLP1 when titrated with Max shows that due to binding of this protein homodimer, DNA curvature is altered. The donor spectrum was normalized in Figure 31 in order to show a better resolution of the acceptor peak. Max when titrated with only fluorescein labeled MLP1 showed a 7-9 % (data not shown) decrease of fluorescence intensity at 520 nm compared to ~60 % decrease of donor intensity in the case of double labeled DNA.

The experiments when repeated with MLP 2 (data not shown) in which we used a different acceptor fluorophore for fluorescein namely TAMRA (Figure 27) in place of ROX and made the distance between donor and acceptor dye pairs further apart (by putting the label on opposite terminus of the two complementary strands in DNA, instead of labeling the either ends of same strand as in MLP1) produced the same result.

The distance between two dyes in free oligos (R_0), in presence of Max (R), actual degree of bending ($R-R_0$), and the bending angle are shown in Table 13.

In order to study the extent to which the bending induced by Max is due to asymmetric neutralization of the charge on DNA's phosphate backbone we repeated the same FRET experiments of FRET with MLP2 and Max in presence of various cationic species like 1mM Spermine, 1mM Spermidine and 5 mM $MgCl_2$. Figure 35 shows the enhancement of acceptor TAMRA peak at 580 of Max binding to MLP2 in the presence of 5 mM $MgCl_2$, the inset shows more enhancement of the acceptor peak caused by Max binding in absence of any cations. Figure 36 show difference in E (energy transfer efficiencies) of MLP2 plotted vs Max concentration in presence and in absence of Spermine and Spermidine. E was calculated using equation *(11, 12)* and the results are tabulated in table 14. For all cationic species E is reduced significantly when Max homodimer binds MLP2.

To observe how the Myc-Max and the Mad-Max heterodimers binding influence the DNA curvature we investigated the change in FRET signal between donor-acceptor dye pairs in MLP1 and MLP2 in the presence of preformed heterodimers. Table 15 shows the R_0 and R values obtained in the case of Myc-Max and Mad-Max binding to MLP1 and MLP2, indicating the absence of significant FRET implying that no bending ocured for the heterodimer binding..

To study the binding affinity of Max with prebent DNA, or rather to find out whether the much tighter binding of Max with DNA compared to Myc-Max or Mad-Max is to some extent due to DNA bending induced by Max, we measured the anisotropy of fluorescein at 520 nm of A tract oligonucleotide (Figure 37) containing the E Box (25). The oligonucleotide is labeled with Fluorescein and TAMRA, like MLP2. The K_{ds} calculated from Equation 5 when compared with that of MLP2, Table 16 showed a 15 fold tighter binding of Max with the prebent A tract.

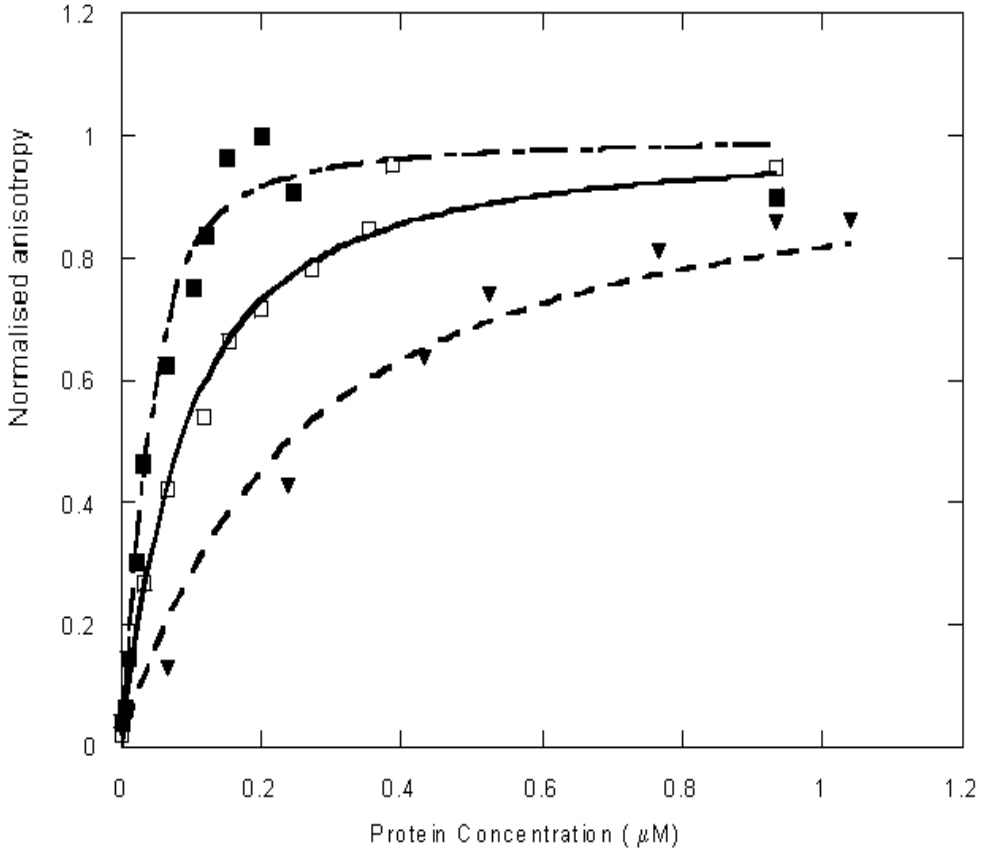

Figure: 29 Titration of 50 nM MLP1 (labeled with fluorescein and ROX) with Max_2 (■), Max-Myc (□), and Max-Mad (▼); anisotropy change of flourescein at 520 nm was observed against protein concentration K_ds are shown in Table 11. Experiment was performed at 23 ºC in 20 mM HEPES-KOH buffer, pH 7.6.

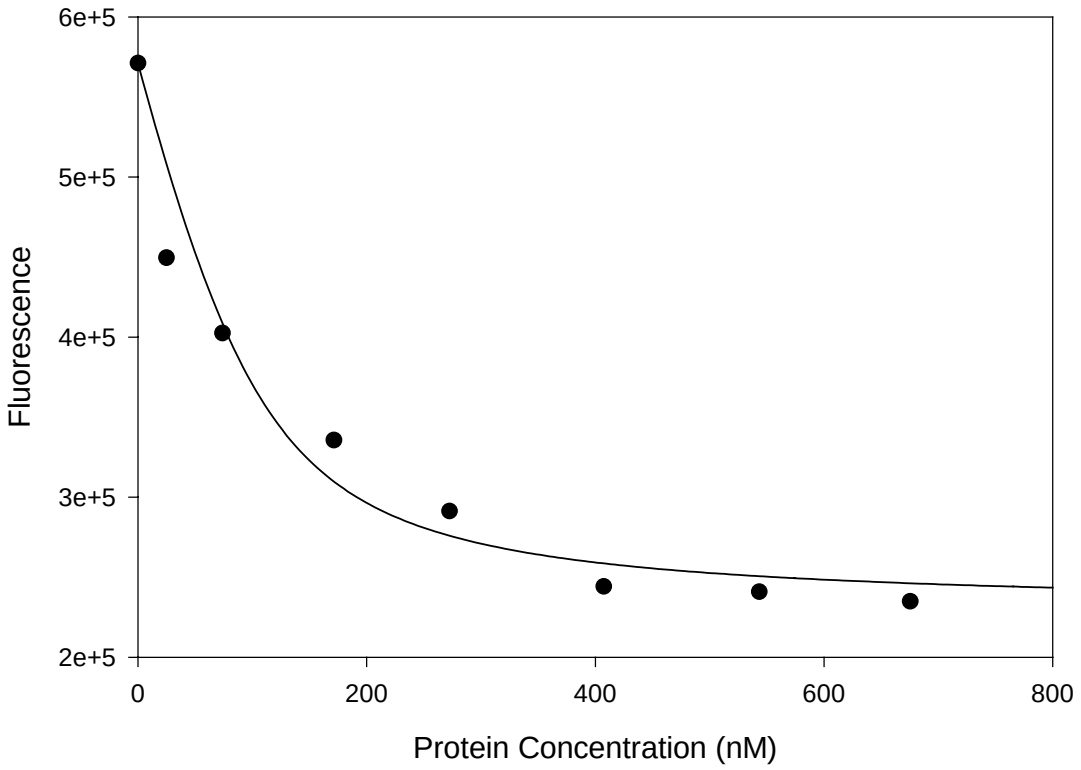

Figure: 30 Titration of 50 nM double labeled MLP1 (labeled with donor fluorescin and acceptor ROX) with 250 nM of Max. (●) Fluorescence intensity decrease of the donor fluorophore, fluorescein at 520 nm was plotted against Max_2 concentration. Dissociation constant K_d was calculated and is shown in Table 10. Experimental conditions were as described in figure 29.

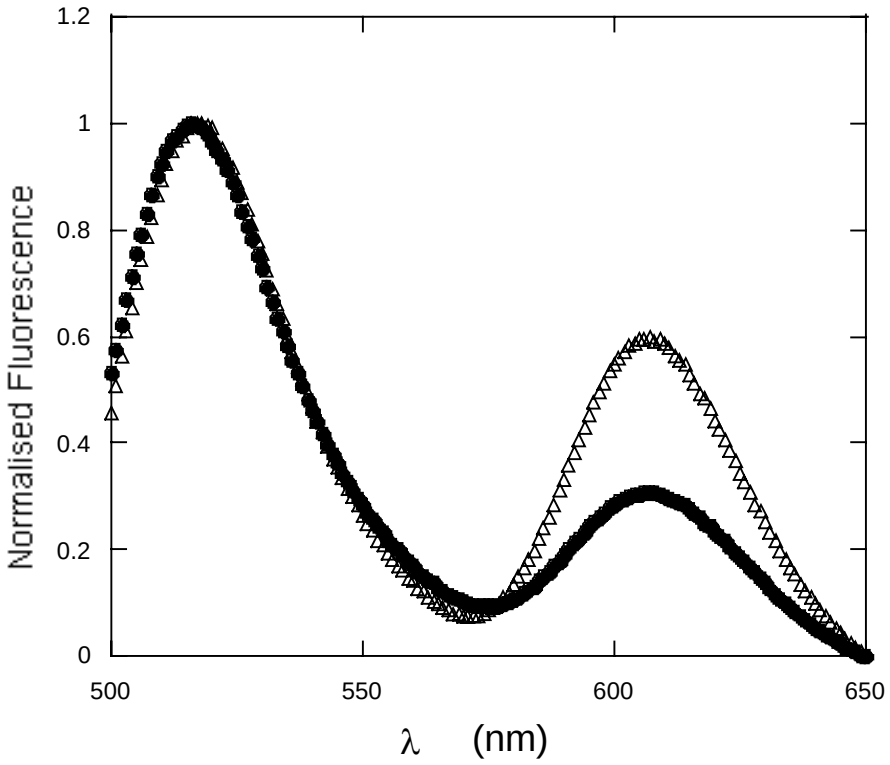

Figure: 31 FRET between ROX and fluorescein in 50 nM MLP1: (●) ROX and Fluorescein labeled MLP1; (Δ): MLP1 + 250 nM Max. Experiment was performed at 23 ºC in 20 mM HEPES-KOH buffer, pH 7.6. MLP1 was excited at 480 nm and decrease in donor fluorescein emission was monitored at 518 (normalized), while enhancement of the acceptor dye ROX was observed at 607 nm.

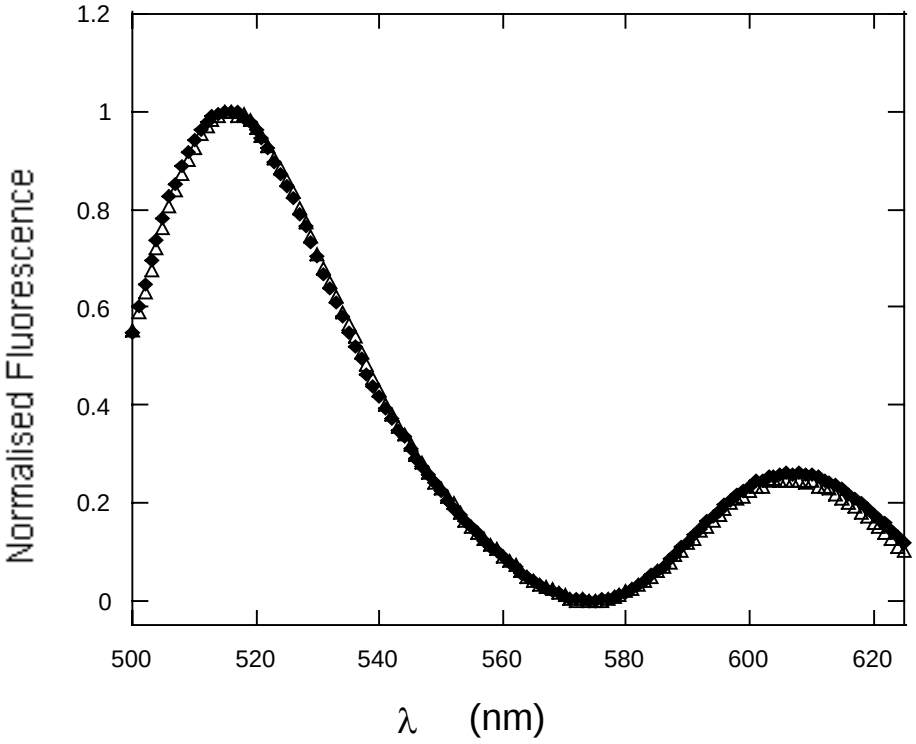

Figure: 32 FRET between ROX and Fluorescin in 50 nM MLP1 in free oligo and in presence of Myc-Max: (■) ROX and Fluorescein labeled oligo MLP1; (Δ): MLP1 + 300nM Max-Myc. Experimental conditions are as described in figure 31.

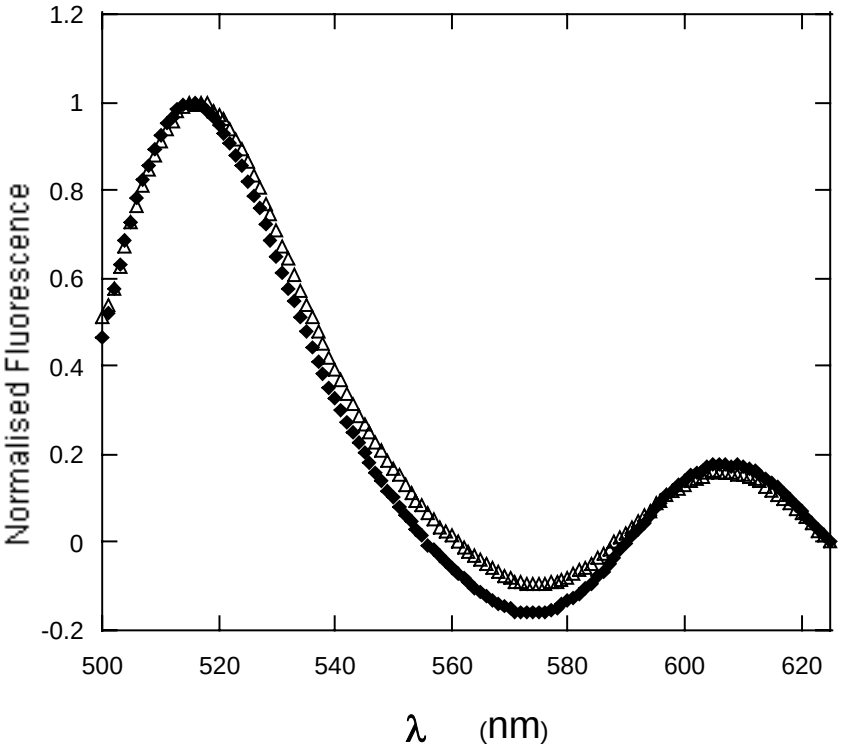

Figure 33:FRET between ROX and Fluorescin in 50 nM free MLP1 oligonucleotide and in the presence of Mad-Max: (■) ROX and Fluorescein labeled MLP1; (Δ): MLP1 + 450nM Mad-Max. Experimental conditions are as described in figure 31..

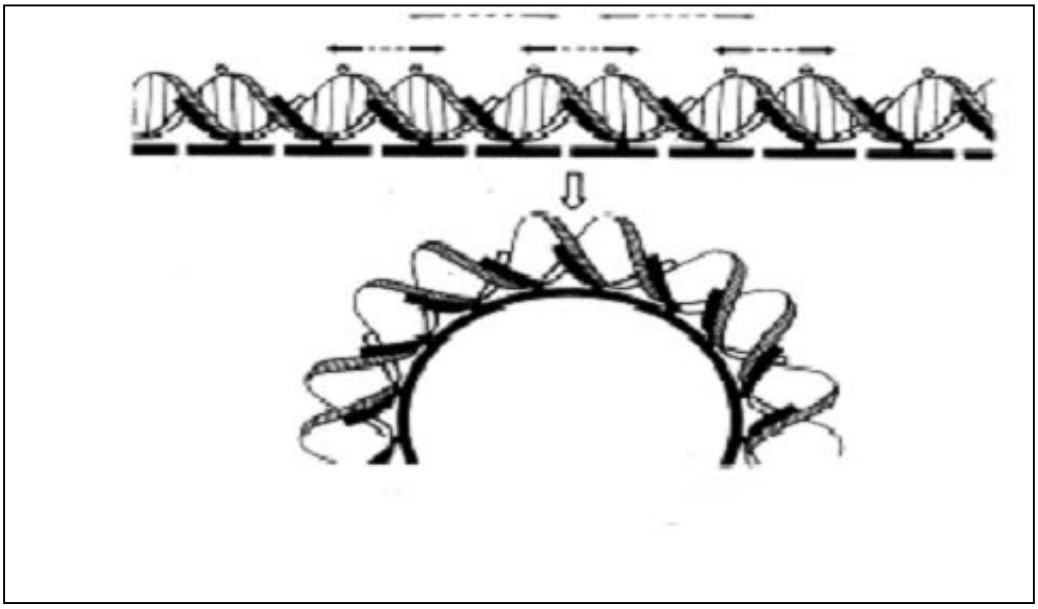

Figure:34 Diagram illustrating the bending of DNA around histone caused by asymmetric neutralization of charges on DNA's phosphate backbone due to histone binding (20).

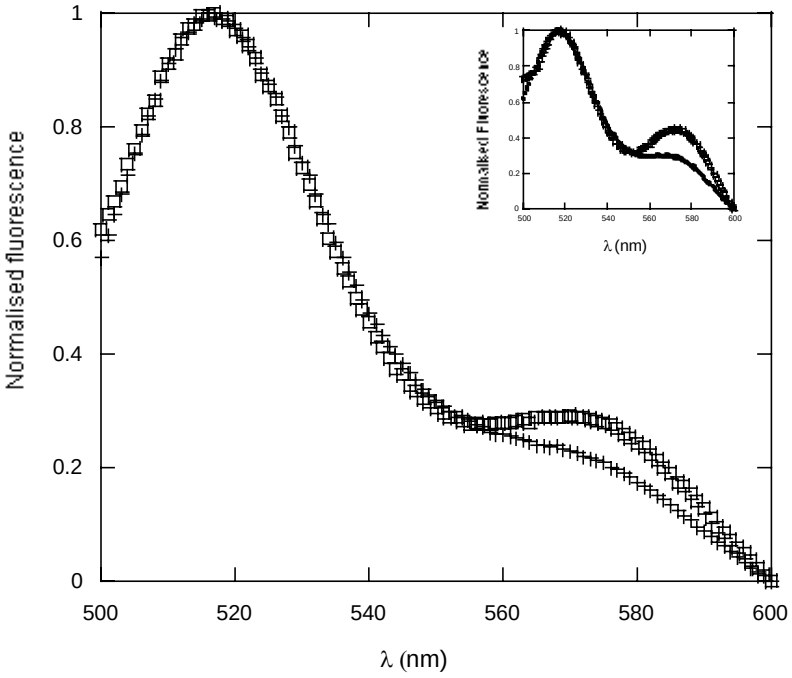

Figure 35 50 nM MLP2 labeled with fluorescein and TAMRA with cationic specie $MgCl_2$ in presence and in absence of 260 nM Max. (+) 5 mM $MgCl_2$. + Free MLP2; (□) 5 mM $MgCl_2$ + Oligo + 260 nM Max .

Inset: 50 nM MLP2 labeled with fluorescein and TAMRA with 260 nM Max.

(●) Free Oligo; (□) Oligo + 260 nM Max. Experiments were performed at 23 ºC in pH 7.6 HEPES-KOH buffer. MLP2 was excited at 490 nm. The emission peak at 520 nm, of the donor dye fluorescein was normalized and the enhancement of the acceptor dye TAMRA at 580 nm was measured for estimating FRET in presence and in absence of cationic speices (in this figure $MgCl_2$).

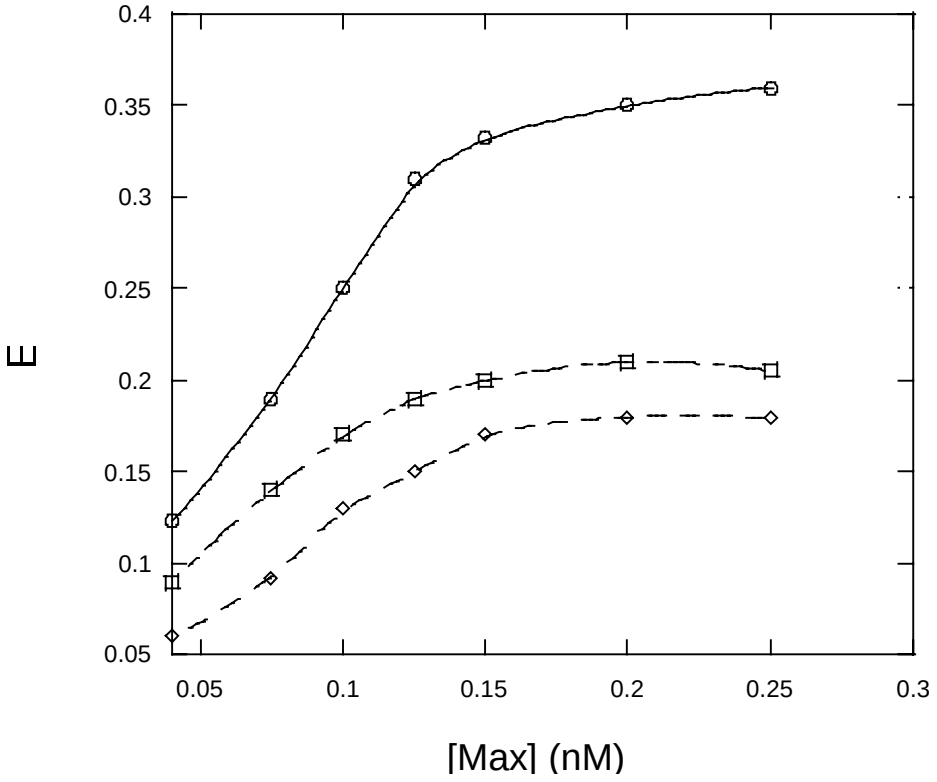

Figure 36 Energy Transfer Efficiency of TAMRA and fluorescein labeled MLP2 titrated with Max in the presence and absence of cationic species. (○) MLP2 + 260 nM Max,; (□)MLP2 + 260 nM Max + 1mM Spermine; (◊) MLP2 + 260 nM Max + 1mM Spermidine. Experiments were performed at 23 ºC in pH 7.6 HEPES-KOH buffer. MLP2 was excited at 490 nm. The emission peak at 520 nm, of the donor dye fluorescein was normalized and the enhancement of the acceptor dye TAMRA at 580 nm was measured for estimating energy transfer efficienct E in presence of cationic speices.

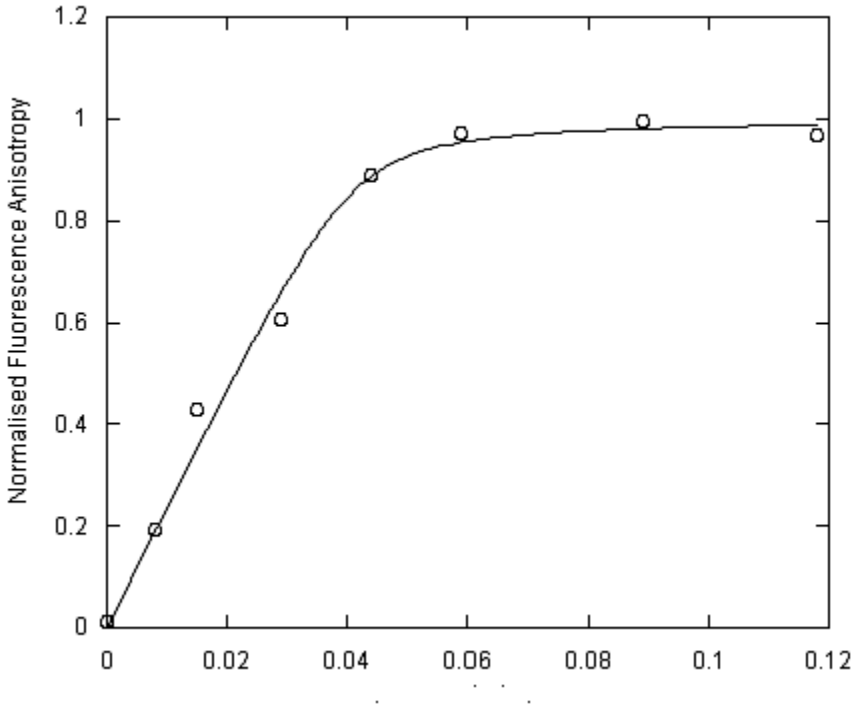

Figure 37 Titration of Max with fluorescein labeled (3' terminus) 50 nM E Box containing A-tract DNA Excitation wavelength was at 490 nm and emission anisotropy was measured at 520 nm. Experiment was performed at 22 ºC in 20 mM HEPES-KOH buffer pH 7.6.

Table 12: Dissociation constants K_{ds} of binding of Max_2, Myc-Max and Mad-Max with MLP1 double labeled oligo measured by change of fluorescence anisotropy of Fluorescein at 520 vs Protein concentration (Figure 29). K_d calculated for binding of Max to MLP1 as a function of decrease of donor Fluorescein during FRET (figure 30) is also shown. The Binding of Myc-Max and Mad-Max heterodimer to MLP1 was not determined by FRET (------) due to absence of any significant decrease in fluorescence intensity of the donor dye, fluorescein

	By Fluorescence anisotropy K_d *(nM)*	*By FRET* K_d *(nM)*
Max_2	14.1±2.4	28.9±5.6
Max-Myc	60.4±5.1	------
Max-Mad	214.6±23	------

Table 13: Energy Transfer data of binding of Max_2 to MLP1 and MLP2 oligos

Oligo Type	*E in free oligo*	*E in oligo + Max_2*	*Donor-acceptor distance in DNA* (R_0)	*Donor acceptor distance in DNA + Max*	*Bending induced by Max binding* (R-R_0)	*Bending Angle (a) Determined by R_0/R =Cos(a/2)*
MLP1	0.31±0.03	0.54±0.07	58.6±1.7Å	49.5±3.5Å	8.6±0.4Å	64.9±3.0°
MLP2	0.17±0.04	0.36±0.06	64.9±1.9Å	55.0±6.0 Å	9.9±1.8Å	63.8±4.6°

Table14: Energy Transfer data of binding of Max to MLP2 in presence of cationic species

MLP2	*Max_2*	*Max_2 + 1mM Spermine*	*Max_2 + 1mM Spermidine*	*Max_2 + 5mM $MgCl_2$*
E	0.36±0.06	0.20±0.03	0.18±0.02	0.23±0.04

Table 15: Energy Transfer data of binding of MLP1 and MLP2 with Myc- Max and Mad - Max

Oligo Type	*E in free oligo*	*E in oligo + Max-Myc complex*	*Donor-acceptor distance in oligo* (R_0)	*Donor acceptor distance in Oligo +Max-*	*E in oligo + Max-Mad complex*	*Donor acceptor distance in Oligo +Max-Mad complex* (R)
MLP 1	0.31±0.03	0.262±0.05	58.6±1.7 Å	60.7±3.4 Å	0.28±0.02	59.7±4.2Å
MLP 2	0.17±0..04	0.141±0.05	64.8±2.0 Å	67.7±1.8 Å	0.15±0.03	66.3±0.4Å

Table 16: Binding of Max compared with MLP1 and A tract double labeled DNA

Max +	MLP1	Atract
K_d(nM)	14.1 ±2.3	0.96 ±0.2

.

2.3. Discussion:

The crystal structure of murine Max dimer (9) and that of Myc-Max and Max-Mad binding to E-box DNA (10) showed that DNA curvature is not altered by binding of these basic helix loop helix proteins. However Brownlie et al (16) published a structure of human Max bound to a 10 base pair E-box containing oligonucleotide in which the DNA was bent about 25 º. Gel based studies have been inconclusive in detecting the presence of bending in DNA bound Max homodimer or Myc-Max heterodimer (7-9).

In our FRET study with MLP1 labeled with ROX and Fluorescein the R_0 of free oligo was altered from 58.6±1.7Å to 49.5±3.5Å creating a total decrease in distance between the dye of 8.6±0.4Å. In order to confirm our result we repeated the experiments with a different fluorescein acceptor probe TAMRA, altered the donor acceptor distance in MLP2. In MLP2 R_0 of the free oligo was 64.9±2Å and R i.e the end to end distance between the fluorophores in protein bound form was 55.0±6 Å. The net bent in DNA due to Max binding in MLP2 was 9.9±1.8Å thus similar to that of MLP1 demonstrating Max induces DNA bending.

The Bending angle was calculated by using the single central bend model (17). The bent was 65 °, which is not consistent with the data published by Brownlie et al (16) in their crystal structure which showed a bend of 25 °. However, in the gel based studies by Fisher et al (8) the bending angles were in the range 75-82°, closer to our data.

DNA is often bent when complexed with proteins and many forces guide this phenomenon (3-5). Understanding the forces responsible for DNA bending is fundamental in exploring the interplay of these macromolecules. One popular hypothesis is repulsions between phosphates in the remaining anionic helix created by neutralization of charges on protein binding surface of the DNA phosphate backbone result in an unbalanced compression force acting to deform the DNA

toward the protein (17-20). This hypothesis is supported by the results of electrophoretic experiments in which DNA spontaneously bends when one helical face is partially modified by incorporation of neutral phosphate analogs (21).

In order to test this hypothesis we repeated the FRET study with MLP2 and Max homodimer in presence of different multivalent cations (24) and also determined the binding affinities of Max towards DNA in presence of those cationic species. Our binding data are in good agreement with our earlier ones in absence of cations (data not shown). In presence of all three cationic species bending of DNA by Max is reduced as shown in figure 34, 35 and table 15.

Figure 29 and table 12 show Myc-Max and Mad-Max bind with double labeled DNA oligos well. However absence of any FRET (Fig 32 for Myc-Max and Fig 33 for Mad-Max) show DNA is not bent in either case. The same result was obtained for MLP2.

Burley and coworkers (10) have reported that for Myc-Max binding to DNA there are several additional H bonding between residues specific to Myc and the phosphate backbone. These bonds are absent in Max homodimer DNA complex. Lys355, Arg356, and two Lysine residues in loop region of Myc Lys371 and Lys392 make both specific and nonspecific H bonding with the phosphate backbone (10). Though for Mad-Max DNA bound structure no such reports are available, similarity in our data of Myc-Max and Mad-Max binding to DNA and presence of homologous conserved residues in Mad suggest that identical contacts might be responsible for absence of any bent in Mad-Max bound form. Thus from our data it could be postulated that Max homodimer is capable of bending DNA helix and this distortion in DNA curvature is at least in part caused by asymmetric neutralization of negative charge on phosphate backbone. Since Myc-Max and possibly Mad-Max bind DNA making additional H-bonding contacts with the backbone phosphates involving residues specific to Myc (or Mad?), DNA bending is not observed in case of the heterodimer-DNA complexes.

Many eukaryotic transcription factors induce DNA bending on binding to their recognition sequences. DNA bending could play a structural role by altering contacts between the protein and DNA, which could be important for the function of transcription regulation (1-3, 26). One hypothesis well tested by Parvin et al. 1995a (22) says if protein binding induces DNA bending, the protein would have higher affinity for prebent DNA. In another study to investigate whether higher binding affinity to prebent DNA could play a more direct role in transcription activation, an intrinsic bent sequence containing continuous stretches of Adenine AAAAAACGTG, was inserted into a minimal promoter containing only a TATA box. The intrinsic DNA bending sequence was a potent activator of transcription in both *in vivo* transfection experiments and in a cell-free transcription system (23).

To investigate the link between the highest binding affinity of Max with DNA compared to Myc-Max and Mad-Max, and presence of bent in Max bound DNA structure, A tract DNA containing intrinsic bent and E Box was titrated with Max (25). The binding affinity was enhanced 15 fold compared to that for MLP1-Max binding (fig 36 and table 16).

Thus our study produced a correlation between DNA bending produced by Max, the role of specific contacts with the phosphate backbone and the protein dimers, and the higher affinity of Max with E-Box, in spite of equivalent amino acid contacts involved to bind E-Box in all three protein-DNA complexes. Our data suggest that directly or indirectly the conformation of the protein-DNA complex is important for transcription. Bending may be necessary to optimize the Max-E box contacts thereby increasing the occupancy of the E-Box in absence of Myc or Mad. The context of the E-box in terms of DNA deformation may play a role in E-box selection.

Appendix

Appendix 1 Buffers and solutions used in the experiments

1.1 Cell media

LB media

NaCl	10g
Yeast Extract	5g
Peptone	10g
+ 1000ml	DDH_2O

1L LB media

SOC media

5M NaCl	2ml
Yeast Extract	5g
Peptone	20g
1M KCl	2.5ml
+	DD H_2O to L

1L SOC media

1.2 Reagents and solutions for cell cultivation

50 mg/ml Ampicillin: 0.5g Ampicillin in 10 ml DD H_2O

50 mg/ml Kanamicin: 0.5g Kanamicin in 10 ml DD H_2O

0.5 M IPTG: 1.62 g IPTG in 12 ml DD H_2O

Protease inhibitor stock

Benzamidine HCl	40 mg
Phenanthroline	25 mg
Aprotinin	25 mg
Pepstatin A	25 mg
Leupeptin	25 mg
1xHEPES buffer	25ml
25ml 100xProtease inhibitor stock	

100mM PMSF: 440mg PMSF in 25ml isopropanol

1.3 Buffers for Protein purification and titrations

10X HEPES Buffer, pH 7.6

HEPES	59.5 g
KCl	74.6 g
$MgCl_2$	2.0 g
DTT*	
DD H_2O	900 ml

Adjust pH to 7.6 by
addition of KOH, then
fill DD H_2O till 1000 ml

* DTT added finally to reach 10 mM

Lysis Buffer

10X HEPES Buffer, pH 7.6	10 ml
Glycerol	10 ml
Protease inhibitor stock	1 ml
100 mM PMSF	1 ml
+78 ml DD H_2O	

100ml Lysis Buffer

Dialysis Buffer (1X HEPES Buffer) 4000 ml

Titration Buffer (1X HEPES Buffer)

1.4 Buffers for Electrophoresis

For DNA Agarose Gel:

50x TAE buffer pH 8.0

Tris base	242 g
EDTA	18.6 g
Glacial Acetic Acid	57.1 ml

Adjust volume to 1L with DD H_2O

6x DNA sample loading buffer

Bromophenol Blue	0.5 ml
1.0%	4.0 ml
Glycerol	0.2 ml
50xTAE buffer	5.3ml
DD H_2O	
Totaling Volume	10 ml

For Protein Gel

10xTank buffer pH 8.8

Tris base	24.22g
SDS	10g
Glycine	144.40g

Adjust volume to 1L with DD H_2O

4x Resolving Gel buffer (1M Tris-Cl buffer pH 8.8)

4x Stacking Gel buffer (0.5M Tris-Cl buffer pH 6.8)

6x Protein Sample Loading buffer

4xStacking Gel buffer	1.56 ml
SDS	1.0 g
Glycerol	5.0 ml
Bromphenol blue	0.5 ml
1.0%	2.5 ml
β-mercaptoethanol	0.44 ml
+ DD H_2O	
Totaling Volume	10 ml

Appendix 2 PROTEIN PURIFICATION AND DETECTING

2.1 Max protein purification by using Hightrap SP column

Gradient Buffers for Hightrap SP column

	Buffer A	Buffer B
2M KCl	6.25 ml	100 ml
10X HEPES Buffer, pH 7.6	50 ml	20 ml
0.5 M EDTA, pH 8.0	0.5 ml	0.2 ml
100 mM PMSF	1 ml (for elution of sample)	1 ml
Glycerol	50 ml	20 ml
Octyl Glycoside	1g (for elution of sample)	1g
DD H_2O	Fill to 500 ml	Fill to 200 ml
Totaling	500 ml	200 ml

Link the Hightrap SP column to the pump.

↓

Run the column with buffer and the sample protein in following sequence

(a) 20 ml Buffer A, 5 ml/min

(b) 50 ml Buffer A, 2 ml/min

(c) 50 ml Buffer A + 1M NaCl, 2 ml/min

(d) 50 ml buffer A, 2 ml/min

(e) Protein Sample, 2 ml/min

(f) 30 ml Buffer A (+ Octyl Glycoside, + PMSF), 2 ml/min

(g) 30 ml 70% Buffer A(21ml) and 30% Buffer B(9 ml) , 2 ml/min

(h) 140 ml 40% Buffer A (56 ml) and 60% Buffer B (84 ml), 2 ml/min

(i) 40 ml 20% Buffer A (8 ml) and 80% Buffer B (32 ml), 5 ml/min

(j) 65 ml Buffer A + 1M NaCl, 5 ml/min

(k) 50 ml Buffer A, 5 ml/min

↓

Collect the fractions eluted in the curve shown in the graph attached to the detector to 1.5 ml tubes (20 drops per tube).

↓

Transfer fractions to dialysis tubing and dialyze against 1X HEPES Buffer overnight in $4^{o}C$.

↓

Estimate protein concentration and detect the purity by SDS-PAGE

↓

Transfer proteins to Centricon Tubes and centrifuge at 5000rpm for 3 hours. Detect the final protein concentration by Bradford methods.

2.2 Mad protein purification by using the His-tag affinity column

The buffers for His-tag affinity column include:

Binding Buffer: 0.5 M NaCl, 20 mM Tris-HCl, 5 mM imidazole, pH 7.9

Wash Buffer: 0.5 M NaCl, 60 mM imidazole, 20 mM Tris-HCl, pH 7.9

Elute Buffer: 1 M imidazole, 0.5 M NaCl, 20 mM Tris-HCl, pH 7.9

Strip Buffer: 0.5 M NaCl, 100 mM EDTA, 20 mM Tris-HCl, pH 7.9

Charge Buffer: 50 mM NiSO4

The protocols used here is as following:

Load 1ml His-Bind resin (from Novagen) to the 5ml sized chromatography column

Load 10 ml of binding buffer to wash the column

Load 5 ml Charge buffer to charge the column with Ni^{2+}

Load 10 ml of Binding Buffer to wash the column

Load the protein samples in Nickel charged His-trap column

Wash the column with 10 ml Binding Buffer

Wash the column with 10 ml Wash Buffer

Elute the column with 10 ml Elute Buffer and start to collect the fractions (20 drops per tubes)

Estimate protein concentration and detect the purity by SDS-PAGE. Transfer fractions with desired proteins to dialysis tubing and dialyze against 1X HEPES Buffer (without DTT) overnight in $4^{o}C$. Transfer proteins to Centricon Tubes and centrifuge at 5000 rpm for 3 hours. Detect the final protein concentration by Bradford methods

2.3 Myc protein purification by GST affinity column

The buffers for GST affinity column include:

10xGST Bind/Wash Buffer: 10x = 43 mM Na2HPO4, 14.7 mM KH2PO4, 1.37 M NaCl, 27 mM KCl, pH 7.3

10xGST Elution Buffer: 10x = 500 mM Tris-HCl, 100mM Reduced Glutathione, pH 8.0

The Protocols used in the experiments are as following:

Gently load 1ml GST•Bind Resin (from Amersham) to small polypropylene columns (5ml size)

Wash the resin with 10ml of GST Bind/Wash Buffer

Load the column with the prepared protein extract

Wash the column with 10ml 1X GST Bind/Wash Buffer.

Elute the bound protein with 5ml of 1X GST Elution Buffer. Collect the fractions (20 drops per tube)

Estimate protein concentration and detect the purity by SDS-PAGE. Transfer fractions with desired proteins to dialysis tubing and dialyze against 1X HEPES buffer (without DTT) overnight in 4^{o}C. Transfer proteins to Centricon tubes and centrifuge at 5000 rpm for 3 hours. Detect the final protein concentration by Bradford method.

2.4 Determine the protein concentration by Bradford Method

The Bradford method to determine protein concentration is by the Coomassie® - Protein Reaction

Protein + Coomassie® G-250 in an acidic medium →protein-dye complex (blue color, measured at 595 nm)

The protocols used in this experiment are as following:

1. Preparation of Diluted BSA Standards

Prepare a fresh set of protein standards by diluting the 2.0 mg/ml BSA stock standard (Stock) (preferably in the same diluent as your samples) as illustrated in TableA.1a below. 1 ml 2.0 mg/ml BSA standard is sufficient to prepare a set of diluted standards for either working range.

Table A.1a: Preparation of the Diluted BSA Standards

Standard Test Tube or Plate Protocol, Working Range = 100 - 1500 µg/ml

Volume of the BSA to Add	Volume of Diluent to Add	Final BSA Concentration
300 µl of (Stock)	0 µl	2,000 µg/ml
375 µl of (Stock)	125 µl	1,500 µg/ml (A)
325 µl of (Stock)	325 µl	1,000 µg/ml (B)
175 µl of (A)	175 µl	750 µg/ml (C)
325 µl of (B)	325 µl	500 µg/ml (D)

325 µl of (D)	325 µl	250 µg/ml (E)
325 µl of (E)	325 µl	125 µg/ml (F)
100 µl of (F)	400 µl	25 µg/ml (G)

2. Mixing of the Coomassie® Plus Protein Assay Reagent

Allow the Coomassie® Plus Reagent to come to room temperature. Mix the Coomassie® Plus Reagent solution just prior to use by gently inverting the bottle several times. Do not shake.

3. Reaction

Pipet 0.05 ml of each standard or unknown sample into an appropriately labeled UV cuvette. Use 0.05 ml of the diluent for the blank. Add 1.5 ml of the Coomassie® Plus Reagent to each tube, mix well.

4.Detection

Switch on the Cary UV linked computer. Open the [Concentration] program on the windows desktop. Measure the absorbance at 595 nm of blank and zero the Cary UV reading. Measure the absorbance at 595 nm of each cuvette. Prepare a standard curve by plotting the average corrected 595 nm reading for each BSA standard versus its concentration in µg/ml. Using the standard curve, determine the protein concentration for each unknown sample.

2.5 SDS Polyacrylamide Gel Electrophoresis (SDS-PAGE)

Assembling gel apparatus according to manufacturer's instructions:

Make gel and pour in the chamber according to the following protocol.

1) Resolving Gels:

Gel concentration of 12% in 0.25 M Tris-HCl pH 8.8

Reagent:	Volume (ml: TO MAKE 5 ML)	Volume (ml: TO MAKE 10 ML)
30% Acrylamide stock*:	2.0	4.0
water (distilled)	1.5	3.2
1 M Tris-HCl pH 8.8	1.3	2.5
10% SDS	0.1	0.2
Ammonium Persulphate	0.1	0.1
10%	5µL	5µL
TEMED (added last)		

* = 29:1 w:w ratio of acrylamide to N,N'-methylene bis-acrylamide

Mix ingredients very carefully in the order shown above, ensuring no air bubbles form. Pour into glass plate assembly. Overlay gel with isopropanol to ensure a flat surface and to exclude air. Wash off isopropanol with water after gel has polymerized (about15 min).

2) Stacking Gels:

Gel concentration of 5% in 0.125 M Tris-HCl pH 6.8

Reagent:	Volume (ml: TO MAKE 5 ML)	Volume (ml: TO MAKE 10 ML)
30% Acrylamide stock*:	0.83	1.66
water (distilled)	2.72	5.54
0.5 M Tris-HCl pH 8.8	1.25	2.5
10% SDS	0.1	0.2
Ammonium Persulphate 10%	0.1	0.1
TEMED (added last)	5µL	5µL

Mix as before, then pour onto top of set resolving gel, insert comb, allow to polymerize (about 30 minutes), remove comb, fill with electrophoresis buffer. Assemble top tank onto glass plate assembly. Fill with electrophoresis buffer.

3) Electrophoresis buffer

The final Tank buffer composition is 196mM glycine / 0.1% SDS / 50mM Tris-HCl pH 8.3, made by diluting a 10x stock solution. This goes in both top and bottom tanks.

4) The protein samples:

Take supernatant and mix 50 µL 1:1 (v:v) with SDS-PAGE disruption mix: this is 125mM Tris-HCl pH 6.8 / 10% 2-mercaptoethanol / 10% SDS / 10% glycerol, containing a little bromophenol blue. For liquid / purified samples, take e.g. 100 µL and add 50 - 100 µL of disruption mix.

Heat sample tubes for 5 min at boiling water in a "float" in a water bath then keep on ice for 10 minutes. Layer samples under buffer into wells on stacking gels. Connect up apparatus and

electrophorese to the power supply. Set voltage as 150V and current as 20mA and run the gel until the blue dye reaches the bottom of the gel.

5) Stain the gel by using Coomassie Brilliant Blue R250

Stain: 0.2% Coomassie Brilliant Blue R250 in 45% 45% 10 % methanol water acetic acid. Cover gel with staining solution, seal in plastic box and leave overnight on shaker (RT) or for 2 to 3 hours at 37 °C also with agitation.

Destain with 25%/ 65%/ 10% methanol water acetic acid mix, with agitation. Change the distaining solution several times until the gel background color becomes transparent.

Appendix 3 SOME MOLECULAR CLONING PROTOCOLS USED IN THESE EXPERIMENTS

3.1. QIAprep Spin Miniprep Kit from Quiagen Protocol to extract and purify the plasmid DNA

The following buffers are applied in this experiment:

Buffers: P1, RNase A has to be added before usage

P2

N3

PB

PE, before use, 24ml ethanol has to be added to obtain 30ml buffer PE

The following protocols are following the QIAprep Spin Miniprep Kit Manual from Quiagen with slight modifications to fit our experiments:

Pellet the 5ml overnight-incubated *E.coli* grown in LB medium by centrifugation at 5000 rpm for 10 minutes.

↓

Resuspend pelleted bacterial cells in 250 µl Buffer P1 (precooled in 4^{o}C) and transfer to a microcentrifuge tube. Ensure that RNase A has been added to Buffer P1. No cell clumps should be visible after resuspension of the pellet.

↓

Add 250 µl Buffer P2 and invert the tube gently 4–6 times to mix. Do not vortex, as this will result in shearing of genomic DNA. If necessary, continue inverting the tube until the solution becomes viscous and slightly clear. Do not allow the lysis reaction to proceed for more than 5 min.

↓

Add 350 µl Buffer N3 and invert the tube immediately but gently 4–6 times. To avoid localized precipitation, immediately after addition of Buffer N3 mix the solution gently but thoroughly. The solution should become cloudy.

↓

Centrifuge for 10 min at 12,000 rpm in microcentrifuge. A compact white pellet will form.

↓

Apply the supernatant from step 4 to the QIA prep Spin Column. Switch on vacuum source to draw the solution through the QIAprep Spin Columns, and then switch off vacuum source.

↓

Wash the QIAprep Spin Column by adding 0.5 ml Buffer PB. Switch on vacuum source. After the solution has moved through the column, switch off vacuum source. This step is necessary to remove trace nuclease activity.

↓

Wash the QIA prep Spin Column by adding 0.75 ml Buffer PE. Switch on vacuum source to draw the wash solution through the column, and then switch off vacuum source.

↓

Transfer the QIAprep Spin Columns to a microcentrifuge tube. Centrifuge for 1 min. This extra spin is to remove residual Buffer PE. Residual ethanol from Buffer PE may inhibit future enzymatic reactions.

↓

Place the QIAprep column in a clean 1.5 ml microcentrifuge tube. To elute DNA, add Nuclease free water to the center of the QIAprep Spin Column, let stand for 1 min, and centrifuge for 1 min.

↓

Take 8 µL of the filtrate and mix with 2 µL DNA sample loading buffer. Load the mix in the 1 % agarose gel containing 1/10,000 dilution of Ethidium Bromide (EtBr) and detect the DNA by EtBr intercalation inUV transilluminator.

3.2. QIAquick PCR Purification Kit Protocol to purify the PCR products

Buffers: PB, PE, before use, 24ml ethanol has to be added to obtain 30 ml buffer PE

The following protocols are following the QIAquick PCR Purification Kit Manual with slight modifications to fit my experiments:

Add 5 volumes of Buffer PB to 1 volume of the PCR sample and mix. For example, add 500 µl of Buffer PB to 100 µl PCR sample.

↓

To bind DNA, load the samples into the QIAquick columns, and apply vacuum. After the samples have passed through the column, switch off the vacuum source. The maximum loading volume of the column is 800 µl. For sample volumes greater than 800 µl simply load again after applying vacuum each time.

↓

To wash, add 0.75 ml of Buffer PE to each QIAquick column and apply vacuum.

↓

Transfer each QIAquick column to a microcentrifuge tube or the provided 2 ml collection tubes. Centrifuge for 1 min at 13,000 rpm. This spin is necessary to remove residual ethanol (Buffer PE).

↓

Place each QIAquick column into a clean 1.5 ml microcentrifuge tube. To elute DNA, add 30 µl of nuclease free water to the center of each QIAquick membrane. Let the columns stand for 1 min, and then centrifuge the columns for 1 min at 13,000 rpm.

3.3. DNA Agarose Gel Electrophoresis

1) Preparation of Agarose solution

To prepare 100 ml of a 0.8% agarose solution, measure 0.8 g agarose into a glass beaker or flask and add 100 ml 1X TAE buffer. Microwave for about 2 minutes until agarose is dissolved and solution is clear.

↓

Allow solution to cool to about 60^{o}C before pouring. 10µl Ethidium bromide (5mg/ml stock) is added to the gel solution at this point to make the final concentration of 0.5 µg/ml.

2) Preparation of Agarose Gel

Prepare gel tray by sealing both ends with tapes. Place comb in gel tray about 1 inch from one end of the tray and position the comb vertically such that the teeth are about 1-2 mm above the surface of the tray.

↓

Pour agarose gel solution into tray to a depth of about 5 mm. Allow gel to solidify about 30 minutes at room temperature.

3) Preparation of DNA samples

Add 1 µl of 6x gel loading dye (see Appendix 1) for every 5 µl of DNA solution. Mix well. Load 5-12 µl of DNA per well.

4) Run the gel

To run, gently remove the comb, place tray in electrophoresis chamber, and cover (just until wells are submerged) with electrophoresis buffer (the same buffer used to prepare the agarose).

↓

Electrophorese at 100 volts until dye markers have migrated an appropriate distance, depending on the size of DNA to be visualized. In this experiments, dye marker only needs to run to the 2/3-gel distance for the PCR products.

5) Detect the result

Place the gel on the transilluminator. Place the clear plastic shield over the transilluminator window before turning on the UV light. Turn on the transilluminator and look at the gel. Confirm the presence of DNA (orange bands) and turn off the transilluminator.

Dispose off the EtBr containing gel in the biohazard container carefully.

3.4. Ligation reaction with Novagen® Clonables 2X Ligation Premix

This kit contains components sufficient for 11 ligation and transformation reactions:

Components: 55 µl Clonables 2X Ligation Premix

10 µl Clonables Positive Control

1.5 ml Nuclease-free Water

11 x 50 µl NovaBlue Singles Competent Cells

2 x 2 ml SOC Medium

1 Test Plasmid

The following procedures are based on the Novagen® Clonables 2X Ligation Premix manual with slight modification to fit our experiment:

The digested pET30a plasmid was purified by using the QIAquick® spin column (protocol in Appendix 3.1)

↓

The digested cDNA PCR product was purified by using the QIAquick® PCR purification column (protocol in Appendix 3.2)

↓

Assembly the ligation reaction mixture as indicated in the table below:

pET30a	1µL
PCR Product	2µL
Nuclease free water	2µL
2xligation premix	5µL
Totaling Volume	10µL

Place the mixture in room temperature for 30 minutes and then place it on ice

↓

Thaw 3 tubes of competent cells (1 tube for negative control, 1 tube for positive control and 1 tube for the ligation products) on ice and mix gently to ensure that the cells are evenly suspended.

↓

Add 1 µl of the ligation reaction directly to the cells. Stir gently to mix. For the positive control, 0.5µL pET30a plasmid is added.

↓

Place the tubes on ice for 5 min. Then heat the tubes for exactly 30 sec in a 42°C water bath; do not shake.

↓

Place the tubes on ice for 2 min. Add 250 µl of room temperature SOC medium to each tube. Shake at 37 °C (250 rpm) for 30 min prior to plating on LB agar containing 30µg/ml kanamycin).

↓

Incubate the plates at 37 °C overnight. Look for single colony.

↓

Pick a few single colonies and with a tooth pick or pipett tip scratch a portion of each colony and do PCR with right primer to check the ligation of the insert.

↓

If PCR is positive, inoculate those single colonies in LB media and begin protein purification.

Bibliography 1:

1. Kohler, J. J. Metallo, S.J, Schneider T.L, Schepartz, A., (1999) *Proc. Natl. Acad. Sci. USA*. **96**, 11735-39.
2. Grandori, C., Cowley, S. M., James, L. P., Eisenman, R. N., (2000) *Annu. Rev. Cell Dev. Biol*. **16**, 653-99.
3. Kato, G. J., Barret, J., Villa-Garcia, M., Dang, C.V., (1990) *Mol. Cell. Biol.* **10**, 5914-20.
4. Murre. C., McCam, P.S., Baltimore, D., (1989) *Cell.* **56**, 777-83.
5. Blackwood, E. M., Eisenman, R. N., (1991) *Science*. **251**, 1211-17.
6. Ayer, D. E., Eisenman, R, N., (1993) *Genes Dev.* **7**, 2110-9.
7. Zervos, A. S., Gyuris, J., Brent, R., (1993) *Cell*. **72**, 223-32.
8. Hurlin, P. J., Queva, C., Koskinen, P. J., Steingrimsson, E., Ayer, D. E., Copeland, N. G., Jenkins, N. A., Eisenman, R. N., (1995b) *EMBO. J.* **14**, 5646-59.
9. Henriksson, M., Luscher, B., (1996) *Adv. Cancer. Res.* **68**, 109-182.
10. Benvenisty, N., Ornitz, D. M., Bennett, G. L., Sahagan, B. G., Kuo, A., Cardiff, R. D., Leder, P., **(**1992) *Oncogene.* **12**, 2399-405.
11. McMahon, S. B., Van Buskirk, H. A., Dugan K. A., Copeland T. D., Cole, M. D., **(**1998) *Cell.* **94**, 363-74.
12. McMahon, S. B., Wood M. A., Cole, M. D., (2000) *Mol Cell Biol.* **20**, 556-62.
13. Amundson, S. A., Zhan, Q., Penn, L. Z., Fornace, A. J. Jr., (1998) *Oncogene.* **17**, 2149
14. Blackwood, E. M., Eisenman, R. N., (1991) *Science.* **251**, 1211-17.
15. Amati, B., Littlewood, T. D., Evan, G. I., Land, H., (1993) *EMBO J.* **12**, 5083-7.
16. Gu, W., Cechova, K., Tassi, V., Dalla-Favera, R., (1993) *Proc Natl Acad Sci U S A*. **90**, 2935-9.

17. Ayer, D. E.; Kretzner, L.; Eisenman, R. N, (1993) *Cell.* **72**, 211-222.

18. McArthur, G. A., Laherty, C. D., Queva, C., Hurlin PJ, Loo L, James, L., Grandori, C., Gallant, Y. S., Hockanson, W. C., Bush, A. C., Cheng, P. F., Lawrence, Q. A., Pulverer, B., Koskinen, P. J., Foley, K. P., Ayer, D. E., Eisenman, R. N., (1998)**.** *Cold Spring. Harbor. Sym. Quant. Biol.* **63**, 423-33.

19. Ferre-D'Amare, A. R., Prendergast, G. C., Ziff, E. B., Burley, S. K., (1993) *Nature.* **363**, 38-45.

20. Nair, S. K., Burley, S. K., (2003) *Cell.* **112**, 193-205.

21. Genetta, T., Ruezinsky, D., Kadesch, T., (1994) *Mol. Cell. Biol.* **14**, 6153-63.

22. Lakowicz, J. R., (1983) *Principles of Fluorescence Spectroscopy*, Plenum Publishing Corp., New York.

23. Sha, M., Wang, Y., Xiang, T., van Heerden, A., Browning, K., Goss, D. J., (1995) *J. Biol. Chem.* **270**, 29904-9.

24. Kohler, J., Schepartz, A., (2001) *Biochemistry*. ***40***, 130-42.

25. Hu, J., Banerjee, A., Goss, D. J., (2005) *Biochemistry*. **44**, 11855-63.

26. Cave, J. W., Kremer, W., Wemmer, D. E., (2000) *Protein Sci.* **9,** 2354-2365.

27. Sha, M., Ferre-D'Amare, A. R., Burley, S. K., Goss, D. J., (1995) *J. Biol. Chem.* **270**, 19325-19329.

28. Blackwell, T. K., Huang, J., Ma, A., Kretzner, L., Alt, F. W., Eisenman, R. N., Weintraub, H., (1993) *Mol. Cell. Biol.* **13**, 5216-5224.

29. O'Hagan, R. C., Schreiber-Agus, N., Chen, K., David, G., Engelman, J. A., Schwab, R., Alland, L., Thomson, C., Roning, D. R., Sacchettini, J. C., Meltzer, P., DePinho, R. A., (2000) *Nat. Genet*. **24**, 113-119.

30. Lavigne, P., Crump, M., Hodges, R. S., Kay, C. M., Sykes, B. D., (1998) *J. Mol. Biol.* **281**, 165-81.

31. Kohler, J. J. Schepartz, A., (2001) *Bio. Org. Med. Chem*. **9**, 2435-5.

32. Rentzeperis, D., Jonsson, T., Sauer, R. T., (1999) *Nat. Struc. Biol.* **6**, 560-73.

33. Berg, T., Cohen, S. B., Desharnais, J., Sonderegger, C., Maslyar, D. J., Goldberg, J., Boger, D. L., Vogt, P. K., (2002**)** *Proc Natl Acad Sci U S A*. **99**, 3830- 3835.

34. Boger, D. L.**, (**2003) *Bioorg Med Chem*. **11**,1607-13.

35. Park, S., Chung, S., Kim, K. M., Jung, K. C., Park, C., Hahm, E. R., Yang, C. H., (2004), *Biochim. Biophys. Acta.* **1670**, 217-228.

36. Fieber, W., Schneider, M. L., Matt, T., Krautler, B., Konrat, R., Bister, K., (2001) *J. Mol. Biol.* **307***,* 1395-410.

37. Subramanin, S., Ross, P. D., (1981) *Biochemistry.* **20**, 3096-102.

38. http://probes.invitrogen.com/handbook/sections/0001.html

Bibliography 2:

1. Kerppola, T. K., (1997) *Biochemistry.* **36**, 10872-84.
2. Diebold, R. J., Rajaram, N., Leonard, D. A., Kerppola, T. K., (1998) *Proc Natl Acad Sci U S A.* **95**, 7915-20.
3. Xiao, J., Singleton, S. F., (2002) *J. Mol. Biol*. **320**, 529-558.
4. Ohndorf, U. M., Rould, M. A., He, Q., Pabo, C. O., Lippard, S. J., (1999) *Nature*. **399**, 708-12.
5. Sitlani, A., Crothers, D. M., (1998) *Proc Natl Acad Sci U S A.* **95**, 1404-9.
6. Maher, L. J 3rd., (1998) *Curr. Opin. Cell. Biol.,* **2**, 688-94.
7. Ramirez-Carrozzi, V. R., Kerpolla, T. K., (2001) *J. Biol. Chem.* **276**, 21797-808.
8. Wechsler, D. S., Dang, C. V., (1992) *Proc. Natl. Acad. Sci. U S A.* **89**, 7635-9
9. Fisher, D. E., Parent, L. A., Sharp, P. A., (1992) *Proc. Natl. Acad. Sci. U S A.* **89**, 11779-83.
10. Ferre-D'Amare, A. R., Prendergast, G. C., Ziff, E. B., Burley, S. K., (1993) *Nature.* **363**, 38-45.
11. Nair, S. K., Burley, S. K., (2003) *Cell*. **112**, 198-205.
12. McCormick, R. J., Badalian, T., Fisher, D. E., (1996) *Proc. Natl. Acad. Sci. U S A.* **93**, 14434-9.
13. Lorenz, M., Hillisch, A., Payet D., Buttinelli, M., Travers, A., Diekmann, S., (1999) *Biochemistry.* **38**, 12150-12158.
14. Clegg, R. M., Murchie, A., Zechel, A., Lilley, D. M., (1993) *Proc. Natl. Acad. Sci. U S A.* **90**, 2994-2998.
15. Kohller, J. J., Schepartz, A., (2001) *Biochemistry.* **40**, 130-42.
16. Wei, C. C., Balasta, M. L., Ren, J., and Goss, D. J., **(**1998) *Biochemistry.* **37**, 1910-6.

17. Brownlie, P., Ceska, T., Lamers, M., Romier, C., Stier, G., Teo, H., Suck, D., (1997) *Structure.* **5**, 509-20.

18. Wu, J., Parkhurst, K. M., Powell, R. M., Brenowitz, M., Parkhurst, L. J., (2001) *J. Biol. Chem.* **276**, 14614-14622.

19. Strauss, J. K., Roberts, C., Nelson, M. G., Switzer, R. C., Maher, L. J.., (1996) *Proc. Natl. Acad. Sci. USA*. **93**, 9515-9520.

20. Williams, L. D., Maher, L. J. 3rd., (2000) *Annu. Rev. Biophys. Biomol. Struct.* **29**, 497–521.

21. Mirzabekov, A. D., Rich, A., (1979) *Proc. Natl. Acad. Sci. U S A.* **76**, 1118-21.

22. Strauss, J. K., Maher, L. J. 3rd., (1994), *Science*. **266**, 1829-34.

23. Parvin, J. D., McCormick, R. J., Sharp, P. A., Fisher, D. E., (1995) *Nature*. **373**, 724-7.

24. Spencer, J. V., Arndt, K. M., (2002) *Mol. Cell. Biol*. **22**, 8744–8755.

25. Curran, T., Kerppola, T. K., (1997) *EMBO. J.* **16**, 2907-2916.

26. Shatzky-Schwartz, M., Hiller, Y., Reich, Z., Ghirlando, R., Weinberger, S., Minsky, A., (1992) *Biochemistry*. **31**, 2339-46

27. Starr, B. D., Hoopes, B. C., Hawley, D. K., (1995) *J. Mol. Biol*. **250**, 434-446.

28. Becker, P. B., (2002) *EMBO. J.* **21**, 4749-753

29. Hu, J., Banerjee, A., Goss, D. J., (2005) *Biochemistry*. **44**, 11855-63.

30. Lorch, Y., Davis, B., Kornberg, R. D., (2005) *Proc. Natl. Acad. Sci. USA*. **102**, 1329-1332.